frontiers | Frontiers in Materials

TYPE Review
PUBLISHED 12 September 2022
DOI 10.3389/fmats.2022.995290

OPEN ACCESS

EDITED BY
Jiefeng Liu,
Guangxi University, China

REVIEWED BY
Hongwei Mei,
Tsinghua University, China
Suting Liu,
Weifang Vocational College, China
Xianhao Fan,
Guangxi University, China

*CORRESPONDENCE
Li Cheng,
chengl16@cqu.edu.cn

SPECIALTY SECTION
This article was submitted to Polymeric and Composite Materials, a section of the journal Frontiers in Materials

RECEIVED 15 July 2022
ACCEPTED 25 August 2022
PUBLISHED 12 September 2022

CITATION
Tao B, Cheng L, Wang J, Zhang X and Liao R (2022), A review on mechanism and application of functional coatings for overhead transmission lines. *Front. Mater.* 9:995290. doi: 10.3389/fmats.2022.995290

A review on mechanism and application of functional coatings for overhead transmission lines

Bo Tao, Li Cheng*, Jiuyi Wang, Xinlong Zhang and Ruijin Liao

State Key Laboratory of Power Transmission Equipment & System Security and New Technology, School of Electrical Engineering, Chongqing University, Chongqing, China

Overhead transmission line is the main method of power transmission. Conductors, insulators, and towers are the primary electrical equipment of overhead transmission lines. Due to overhead transmission lines work in the natural environment, problems such as icing, corona discharge, contamination deposition, and corrosion will arise. As a result, some accidents may occur, which cause enormous economic losses. The above problems can be solved by coating functional coatings with superhydrophobic, semiconductive, anti-corrosion, and other characteristics on electrical equipment, which has the advantages of low cost and high efficiency. Therefore, functional coatings have become a research hotspot in the field of external insulation in recent years. In view of the various problems of different electrical equipment in overhead transmission lines, distinctive solutions need to be adopted, so this review classifies the coatings according to the usage scenarios and functions. In each category, first briefly outlines the causes of the electrical equipment problem, then introduces the mechanism of using this type of functional coating to solve the problem, next summarizes the development and application status of this type of coating, after summarizes the limitations of this coating, and finally provides a summary of the key issues in the research of functional coatings and gives an outlook on potential future research directions. This review intends to provide readers with a comprehensive overview of the performance principles and current application status of functional coatings for overhead transmission lines.

KEYWORDS

functional coating, superhydrophobic, anti-icing, anti-corona, anti-pollution flashover, anti-corrosion, overhead transmission lines

1 Introduction

Transmission line is the medium of power transmission, which includes overhead transmission lines, cable transmission lines, gas-insulated transmission lines (GIL). In 1882, the first long-distance (about 57 km) 2 kV (very high voltage at the time) overhead transmission line between Miesbach and Munich was commissioned successfully (Guarnieri, 2013). Since then, the technologies associated with overhead transmission lines have been developed rapidly. By 1985, the Soviet Union successfully built a 1,150 kV overhead transmission line between Elektrostal and Ekibastuz, with a total length of

TABLE 1 Representative functional coatings for overhead transmission lines.

Electrical equipment	Problems	Functional coatings
Conductor	Conductor icing	Superhydrophobic coatings
		Electrothermal coating
		Photothermal coatings
	Conductor corona	TiO_2 coatings
		Superhydrophobic coatings
	Conductor corrosion	Anti-corrosion greases
Insulator	Insulator contamination	Superhydrophobic coatings
		Nonlinear coatings
		TiO_2 coatings
	Insulator icing	Semiconductive coatings
		Superhydrophobic coatings
		Coatings with phase change material
Tower	Tower corrosion	Anti-corrosion coatings

432 km and a maximum transmission capacity of 5,500 MW (Li et al., 2020a). Overhead transmission lines have irreplaceable advantages such as wide applicable voltage levels, low construction costs, easy maintenance. Therefore, overhead transmission lines have become the most mature and mainstream power transmission method. In overhead transmission lines, conductors, insulators, and towers are the basic electrical equipment. Conductors are the carriers of power transmission; insulators provide mechanical support and electrical insulation; towers are utilized to support lines, insulators, and other accessories. As overhead transmission lines work in the natural environment, they need to withstand the test of wind, Sun, rain, snow, frost, and contamination deposits. Problems such as conductor icing, conductor corona, conductor corrosion, insulator contamination, insulator icing, and tower corrosion have a significant negative impact on the stable operation of transmission lines and may lead to conductor breakage, tower collapse, tower base damage, and large-scale power outages, resulting in substantial economic losses (Farzaneh et al., 2015). For instance, in January 2008, a rain, snow, and freezing disaster occurred in southern China, and the overhead transmission lines were severely covered with ice, resulting in the collapse of 1,325 towers of 220 kV and above, and the breakage of 2,129 conductors (Zhao et al., 2022), with direct economic losses exceeding $3.5 billion (Farzaneh et al., 2008). In February 2021, an extreme winter storm swept across the United States, icing the Texas power grid seriously and disrupting power supply to more than 4.5 million people (Menati and Xie, 2021). Therefore, solving the aforementioned overhead transmission line problems is of great significance to the stability of transmission lines and minimizing economic losses.

The use of coatings to improve the performance and stability of the electrical equipment of overhead transmission lines has a long history. As early as 1927, vaseline was coated on conductor joints for anti-corrosion for the first time in the United States (Xu, 2015). Since 1970, RTV anti-pollution flashover coatings have been widely used to improve the pollution flashover performance of glass and ceramic insulators (Karady et al., 1995). With the development of organic material science and nanoscience, more and more functional coatings with superior performance have been produced. Functional coatings refer to coatings with superhydrophobic, self-cleaning, semiconductive, and anti-corrosion capabilities. Some representative functional coatings are shown in Table 1.

In many scenarios, the use of functional coatings to solve overhead transmission line problems has irreplaceable advantages. For example, the superhydrophobic coating applied to conductor anti-icing has the advantages of low cost, high efficiency, and light weight compared with existing methods such as DC ice melting and mechanical deicing; the use of anti-pollution flashover coatings on insulators can eliminate the tedious steps of manual cleaning of insulators and greatly reduce transmission line maintenance costs. It is precisely because functional coatings exhibit unique advantages such as low cost, high efficiency, low energy consumption, and light weight, and are expected to become the preferred solution for transmission line problems. Unfortunately, only a few functional coatings have been successfully commercialized. This is because the current functional coatings still have some common problems, such as high cost of coating preparation, poor wear resistance, and short coating life, which seriously affect their reliability and feasibility, hindering the large-scale application of functional coatings. More and more studies have also paid attention to these problems, strengthening the research on optimizing the coating preparation method and improving the coating durability.

This review briefly reviews the causes of the primary electrical equipment problems in transmission lines, the performance mechanism of functional coatings, coating preparation methods, and coating limitations in Table 1. The key issues in the research of functional coatings for transmission lines are summarized, and the possible research directions of functional coatings are briefly described.

2 Coatings of conductors

2.1 Coatings aim at conductors icing

Under suitable atmospheric conditions, icing can form on overhead lines (including conductors and ground lines), and the typical accretion loads of icing lines is 325 kg/m, and even higher

in extreme conditions (Farzaneh et al., 2015), which can cause an increase in mechanical loads on transmission lines. At the same time, icing will change the aerodynamics of the lines, which are prone to galloping under the influence of wind excitation, causing the line to jump during the de-icing period and even leading to serious accidents such as large-scale power outages, collapse of towers, and disconnection of lines. Consequently, resolving the issue of line icing is crucial for the reliable operation of overhead transmission lines and the reduction of economic losses.

Current methods for line icing are mostly separated into two categories: anti-icing and de-icing. The use of functional coatings such as superhydrophobic, electrothermal, and photothermal for conductors anti-icing offers the advantages of low energy consumption, light weight, and high efficiency when compared to other anti-icing and de-icing technologies (Cao et al., 2022), showing the potential for a wide range of applications (Farzaneh et al., 2015).

2.1.1 Superhydrophobic coatings

The superhydrophobic surface (SHS) has a static contact angle (SCA) greater than 150° and a sliding angle less than 10°. Three aspects can be used to describe the anti-icing mechanism of superhydrophobic surfaces: First, the superhydrophobic surface has a low sliding angle, allowing water droplets to bounce and detach from the surface before freezing. Second, the water droplets will form a Cassie-Baxter model on the superhydrophobic surface, and the rough structure will act as air pockets to capture air to form a good thermal insulation layer, reducing heat exchange between the water droplets and the surface and thus delaying water droplet nucleation time (Tourkine et al., 2009). The third is that due to the low adhesion of ice on superhydrophobic surfaces (usually less than 100 kPa), ice can be easily removed by natural forces (Boinovich and Emelyanenko, 2013).

Because the overhead lines are mostly aluminum conductors, here will focus on work carried out on aluminum substrates. The fabrication of superhydrophobic coatings on aluminum substrates can be divided into one-step and two-step. One-step refers to directly forming a superhydrophobic coating on the aluminum substrate by dip coating, spray coating, drop coating and other methods. Yang et al. (2015) developed a ZnO/PDMS superhydrophobic coating with the SCA of 159.5° and a sliding angle of 8.3°. When the surface is inclined at 10° at temperatures ranging from −5°C to 10°C, water droplets entirely slide off the SHS, which has excellent anti-icing performance. The SCA of the sample is still larger than 150° after ten icing/deicing tests, the sliding angle does not change significantly, the coating durability is good, and the self-healing phenomenon of the coating is also observed. Tan et al. (2021) used polyvinylidene fluoride (PVDF) and SiO_2 to prepare a superhydrophobic coating via one-step dip coating, the SCA was 159°, the sliding angle was 3°, and the use of superhydrophobic coating extended the freezing time 4 times, the adhesion of ice on the aluminum sheet is reduced by 40%. At the same time, the coating possesses excellent weather resistance, acid and alkali corrosion resistance, and high temperature resistance.

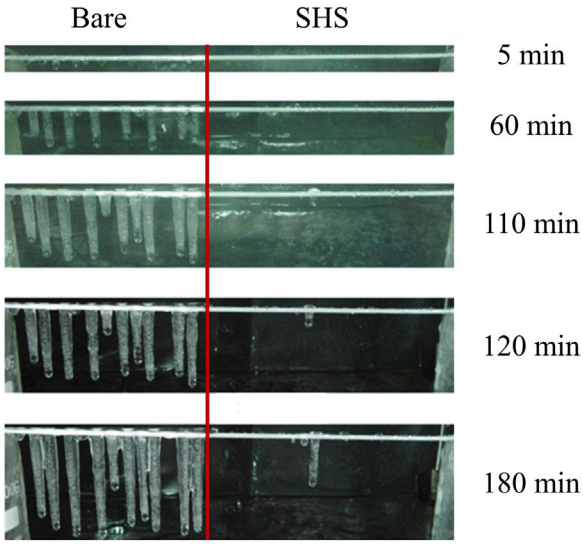

FIGURE 1
The icing process on the conductor in the icing simulation test (the left side of the red line is the untreated conductor, and the right side is the prepared superhydrophobic conductor) (Jin et al., 2018).

The two-step is divided into two steps: first, the aluminum substrate is preproced using chemical etching (Liao et al., 2014; Jin et al., 2018; Fenero et al., 2020; Lo et al., 2021), magnetron sputtering (Zuo et al., 2019; Liu et al., 2020a), anodizing (Liu G. et al., 2021), femtosecond laser (Volpe et al., 2020), and other methods. The goal of preprocessing is to prepare micro-nano structures. Then, *via* immersion (Liao et al., 2014; Zuo et al., 2019; Liu et al., 2020a; Fenero et al., 2020; Lo et al., 2021), chemical vapor deposition (Cao et al., 2022), physical vapor deposition, and other methods for low surface energy hydrophobic modification. Liao et al. (2014) continuously chemical etched aluminum substrates using $CuCl_2$ and HCl, then modified them with silane. The prepared SHS has the micro-nano composite structure, SCA is 161.9° ± 0.5° and the sliding angle is 6.8° ± 1°, and about 53% of the surface remained unfrozen after 50 min in the glaze icing test. Jin et al. (2018) prepared a SHS with a SCA of 159° and a sliding angle of 6° on conductors by using the preferential etching theory of crystal defects. In the line icing test at a temperature of −25°C and a relative humidity of 85%. Because the synergistic effect of the superhydrophobic rough surface and low surface energy, the quantity and average length of ice picks of the prepared conductors are significantly smaller than the untreated aluminum conductors. As shown in Figure 1, it can be seen

that the prepared superhydrophobic conductors exhibit exceptional anti-icing performance. Zuo et al. (2019) prepared a SHS on the surface of aluminum sheets by magnetron sputtering and silane modification, which consisted of a nanostructured ZnO layer and a low surface energy hexadecyltrimethoxy silane (HDTMS) molecular layer. At 60 min, just 24.65% of the SHS was covered with ice during the glaze icing test. Fenero et al. (2020) prepared an omniphobic surface *via* chemical etching the aluminum sheet with $FeCl_3$ and grafting PTFE molecules onto the surface. In the low-temperature freezing test at −5°C and relative humidity of 50% ± 5%, the freeze time of water droplets on the omniphobic surface is 20 times longer than the untreated aluminum sheet. Liu et al. (2020b) used magnetron sputtering to fabricate a ZnO SHS on an aluminum sheet. Sputtering for 15 min can obtain a micro-nano rough structure consisting of densely aggregated nanoclusters. Experiments reveal that the freezing delay of water droplets on SHS is approximately 2 h, the frosting delay of SHS is approximately 5 h at −10°C, and the adhesion of ice on SHS is only 12 ± 4.7 kPa. The fabricated ZnO SHS has excellent anti-icing and anti-frost properties.

Kulinich et al. (2011) noted that the mechanical stability of the micro-nano structure on the superhydrophobic surface is extremely low. With the increase of icing/deicing times, the micro-nano structure will be severely damaged, resulting in a sharp decline in the SHS's anti-icing properties. Therefore, conducting experimental studies on the endurance of superhydrophobic coatings is of major importance. Lo et al. (2021) constructed a micro-nano hierarchical rough structure on the surface of an aluminum plate using chemical etching and hot water treatment, and coated it with low surface energy polydimethylsiloxane (PDMS) and 1H, 1H, 2H, 2H-heptadecafluorodecyl (FD). The SCA of the prepared SHS is 175°, the sliding angle is 1.5°, and the ice adhesion is 25.3 kPa. In addition, the ice adhesion is 47.2 kPa after 100 icing/deicing cycles. It can be noticed that the anti-icing surface has excellent durability, which may be due to the pliability of PDMS. Liu J. et al. (2021) prepared a durable superhydrophobic anti-icing surface on the surface of aluminum sheet by anodizing and silanization modification. After 30 icing/deicing cycles, the ice adhesion remained below 70 kPa and the SCA remained above 150°. Cao et al. (2022) developed superhydrophobic anti-icing coatings (F-SiO_2 coatings) on aluminum sheets and conductors utilizing soot template method and chemical vapor deposition method, the SEM images are shown in Figures 2A,B. The icing delay time on the superhydrophobic anti-icing coating is 9.75 times that of the untreated aluminum plate in the droplet freezing test at −10°C and a relative humidity of about 85%. The adhesion of ice on the surface of the superhydrophobic coating is 14.8 kPa. At the same time, the coating still maintains anti-icing performance after 150 icing/deicing cycles. In the simulated conductor icing test, the coated and uncoated conductor were first kept at −10°C for 30 min, and then water droplets at 0°C were dropped on the conductor. The coated conductor did not start to freeze until 270 s, the test results are shown in Figures 2C,D.

There is no report on the large-scale usage of superhydrophobic coatings for anti-icing of overhead lines due to the restrictions of low coating durability, difficult preparation procedure, and high production costs. Notably, Liu G. et al. (2021) achieve that the ice can self-shed under the action of torque *via* increasing the string tension, installing anti-torsion devices, and coating with a hydrophobic coating (not a superhydrophobic coating). This is instructive for the anti-icing application of superhydrophobic coatings on conductors.

2.1.2 Other coatings

In addition to superhydrophobic anti-icing coatings, anti-icing solutions based on Slippery Liquid Infused Porous Surfaces (SLIPS) (Kim et al., 2012; Liu et al., 2015, Liu et al., 2020b, Liu et al., 2022), photothermal coatings (Jiang et al., 2018; Liu Y. et al., 2021), and electrothermal coatings (Wang et al., 2020; Liu J. et al., 2021) exhibited distinctive benefits.

2.1.2.1 Slippery liquid infused porous surfaces

Kim et al. (2012) fabricated SLIPS on aluminum sheets by infiltrating 3–4 μm thick polypyrrole films prepared by oxidative electrochemical deposition with a low-viscosity perfluorinated lubricant. At −10°C, the adhesion of ice on the treated aluminum sheet was only 15.6 ± 3.6 kPa. Liu et al. (2015) used the electrospray method with phase separation to prepare a graded microstructured silicone rubber surface on aluminum plates, and then injected perfluoropolyether lubricant to obtain SLIPS with a SCA of 162.6° ± 5.8° and a contact angle hysteresis of ~0°. In frosting/defrosting cycle test, ice adhesion increases gradually as lubricant loss. Liu et al. (2020a) utilized anodization to create nanopores with a diameter of 88 nm and a pore depth of 20 μm on the surface of aluminum plates, and then injected low-viscosity silicone oil with different viscosities to fabricate SLIPS. Compared with the bare aluminum plate, the SLIPS adhesion of ice injected with 10 mPa s silicone oil was reduced by 99.3% to only 2.7 kPa. After 21 icing/deicing cycles, the SLIPS injected with 50 mPa s silicone oil exhibited the best durability, the ice adhesion was still 10% of the bare aluminum plate. Liu et al. (2022) fabricated anti-icing SLIPS with self-healing characteristics by injecting fluorosilane (FAS-17) into the pores created by anodization on aluminum plates, SCA is 165.9° ± 1.7° and the sliding angle is 0.6° ± 0.3°. In the glaze icing test, the SLIPS aluminum plate did not freeze after 80 min, and the test results are shown in Figure 3A. The SCA of the SLIPS aluminum sheet reduced to 156.3° ± 3.1° after the 7.68 m abrasion experiment. However, after 30 min self-

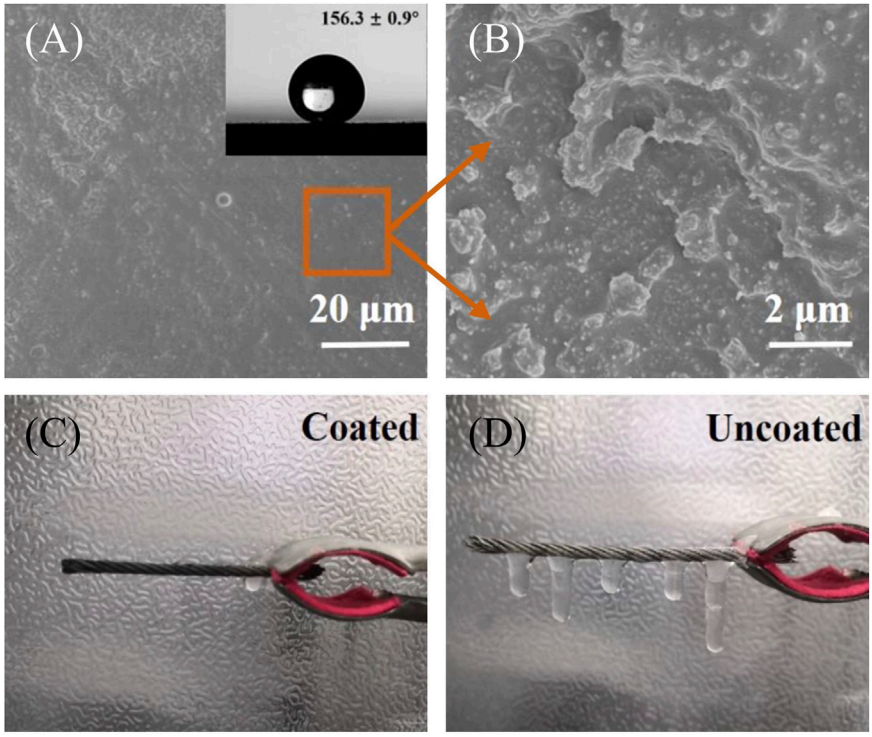

FIGURE 2
SEM images of **(A,B)** the over and the partially-enlarged views of the F-SiO_2 coating (Cao et al., 2022). **(C,D)** Test of anti-icing performance simulated conductor (Cao et al., 2022).

healing at 70°C, the SCA recovered to 165.1° ± 2.1°. Figure 3B shows the self-healing process. The SEM images of 7.68 m abrasion experiment are shown in Figure 3C, and it can be seen that the pore structures produced by anodization are still maintained.

2.1.2.2 Photothermal coatings and electrothermal coatings

Jiang et al. (2018) prepared a photothermal/superhydrophobic SiC/CNTs coating with a SCA of 161° and a sliding angle of 2° by spraying. Under near-infrared light (808 nm) irradiation, the surface temperature increased from 30°C to 120°C within 10 s, enabling quick deicing. Wang et al. (2020) proposed an electrothermal/superhydrophobic synergistic anti-icing method based on graphene composites. After turning off the DC power source, a tiny quantity of ice would form on the surface. However, after applying 50 V voltage, the ice can be quickly removed within 70 s. Liu G. et al. (2021) prepared photothermal/electrothermal/superhydrophobic coatings composed of conductive carbon nanotubes (ECNTs) and fluorine-modified polyacrylates by simply spraying method for All-Day anti-icing and de-icing ice.

Lastly, the performance comparison of some typical functional coatings aim at conductors icing are shown in Table 2.

2.2 Coatings aim at conductors corona

For transmission lines to fulfill the power demands of load centers, the voltage levels are gradually rising. When the electric field strength on the surface of the conductor is sufficient, the air surrounding the conductor will be ionized and corona discharge will occur. Corona discharge has numerous negative consequences, such as corona loss (CL), radio interference (RI), audible noise (AN), and air ionization to produce ozone, among others. Corona loss computation is the primary work for the optimal design of overhead transmission lines and plays a crucial role in the design of high-voltage long-distance transmission lines in high altitude areas (Maruvada, 2000). Under meteorological conditions such as rain, snow, and fog, many water droplets will appear on the surface of the conductor, which will deform into a cone under the action of electric field and gravity, distort the electric field on the surface of the conductor, lower the corona inception voltage, and increase the corona loss of the line (Pfeiffer and Franck, 2015). It is important to note that there are some differences between alternating current (AC) and direct current (DC) corona due to the different motion behavior of space charge. The maximum levels of RI and AN for AC lines occur in bad weather, while for DC lines in good

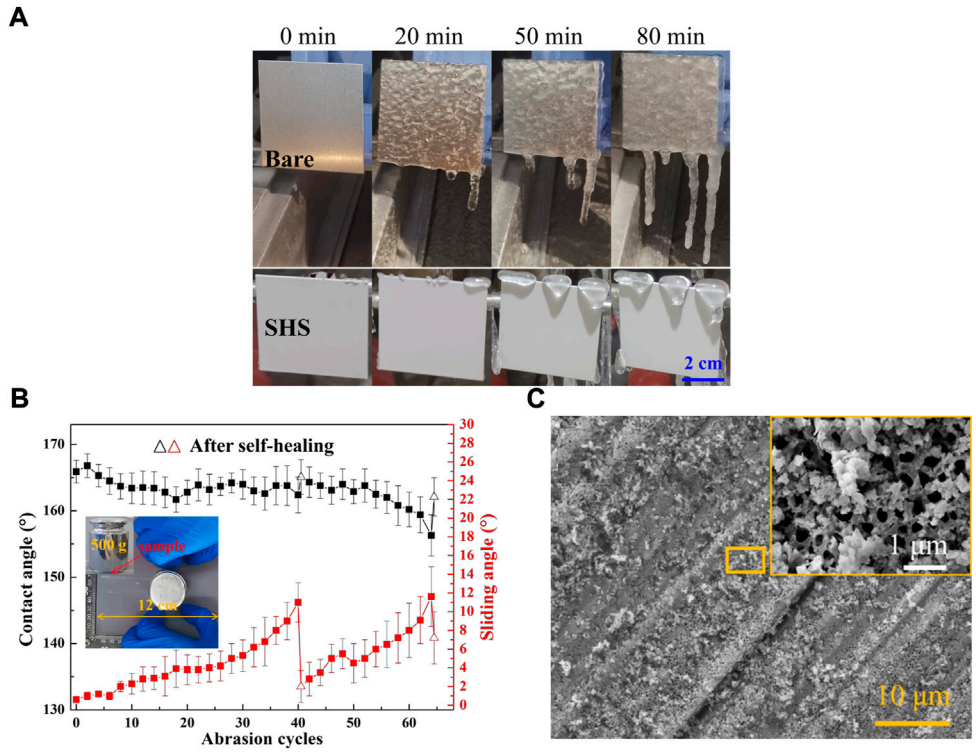

FIGURE 3
(A) The images of ice formation on bare Al plate and the as-prepared SHS (Liu et al., 2022). **(B)** Contact angle and sliding angle for water on the SHS after abrasion cycles and self-healing treatment (Liu et al., 2022). **(C)** The SEM images of the SHS after being abrasion for 7.68 m. The inset was the larger magnification (Liu et al., 2022).

weather (Hylten-Cavallius et al., 1964). In addition, for DC lines, suspended particles with opposite polarity charged will attach to the conductor surface, increasing the surface roughness and reducing corona inception voltage (Jie et al., 2020).

The key to solving the corona discharge problem is to homogenize or reduce the electric field strength on the wire surface (Maruvada, 2000). Methods such as increasing the diameter of the conductors, using bundle conductors, increasing the phase-to-phase spacing, or increasing the height of the tower can reduce the corona loss of the overhead transmission line, but the above methods will greatly increase the construction cost. In recent years, researchers have proposed many anti-corona coatings, which are expected to solve the corona problem. There are mainly hydrophobic coatings (Xu and Li, 2013; Yi et al., 2016; Zhang et al., 2019), TiO_2 coatings (Bian et al., 2018; Xu et al., 2022), and high dielectric coatings (Megala and Sugumaran, 2019; Megala and Pugazhendhi Sugumaran, 2020).

The conductors are coated with hydrophobic and superhydrophobic coatings to prevent water droplets adhering to the conductors, thereby reducing the electric field distortion caused by water droplets. Xu and Li (2013) directly coated a 22.82 mm diameter cylindrical steel rod with a 1 mm thick RTV coating, and the AC corona loss was only about 40% of that of the bare steel rod. Yi et al. (2016) found that the DC corona inception voltage increases with the thickness of the RTV coating on the aluminum conductor steel reinforced (ACSR). Zhang et al. (2019, 2022) applied a commercial superhydrophobic coating on ACSR, the SCA was 162.4°. The application of the superhydrophobic coating greatly reduces the quantity of droplets on the ACSR and reduces the electric field distortion generated by the tip of the water droplet. The UV camera images in Figures 4A,B demonstrate that the corona discharge has decreased dramatically. As shown in Figures 4C,D, the application of the superhydrophobic coating increases the corona inception voltage by 27% and decreases the audible noise output (power) by about 33%–44%.

The TiO_2 coating exhibits photoinduced superhydrophilic and photocatalytic characteristics. Photoinduced superhydrophilicity can make the water droplets spread evenly on the surface of the conductor, thereby reducing the electric field distortion caused by the water droplets. Photocatalysis can decompose the contamination, reduce the surface roughness of the conductor, and reduce the surface electric field distortion.

TABLE 2 Performance comparison of typical researches about functional coatings of conductors icing.

Type	Wettability [static contact angle (SCA) and sliding angle (SA)]	Anti-icing performance (icing delay time, unfrozen area, Adhesion of ice, etc.)	Durability (result of icing/deicing test, Sandpaper Abrasion test, etc. tests)	References
Superhydrophobic coatings				
One-step	SCA 159.5° SA 8.3°	−10°C, icing delay time ~1,380 s	After 10 icing/deicing tests, SCA >150°	Yang et al. (2015)
	SCA 159°, SA 3°	6 h glaze icing test, mass of ice decline 71.4%	After 18 icing/deicing tests, SCA 148°, SA 13.5°	Tan et al. (2021)
Two-step	SCA ~161.9°, SA ~6.8°	50 min glaze icing test, 53% surface unfrozen	After 5,000 droplets 50 μl 40 cm water-drop test, SCA 155.7 ± 2.3°	Liao et al. (2014)
	SCA ~171.8°, SA < 1.5°	−10°C, icing delay time >2000 min	After 100 icing/deicing tests, SCA >162°, SA < 15°	Boinovich et al. (2019)
Slips	SCA ~162.6°	−20°C, adhesion of ice ~60 kPa	After 100 icing/deicing tests, lubricant retention rate ~37%	Liu et al. (2015)
	SCA ~165.9°, SA ~0.6°	80 min glaze icing test, most surface are unfrozen	After 12 kPa 7.68 m 1,000 cW sandpaper abrasion, SCA >156°, SA ~11.6°, but prepared SLIPS can self-heal	Liu et al. (2022)
Photothermal coatings	SCA 161°, SA <2°	−30°C 30% RH, adhesion of ice 2.65 kPa Under NIR irradiation, temperature increased from 30°C to 120 °C within 10 s	—	Jiang et al. (2018)
Electrothermal coatings	SCA 167°, SA 2°	−5°C, icing delay time 335 s In glaze icing test, applied 50 V, temperature of coating increased to 70°C, 3 mm thick ice can be removed in 70 s	After 500 g 8 m sandpaper abrasion, SCA >150°, SA < 10°	Wang et al. (2020)

Bian et al. (2019) coated the conductor with a silicon acrylicresin coating with nano-TiO_2. The coating has the characteristics of high relative permittivity and hydrophilicity, which can reduce the surface electric field strength and increase the DC corona inception voltage. At the same time, because of the photoinduced superhydrophilic of TiO_2, the contact angle will be further reduced under the condition of ultraviolet light. Xu et al. (2022) prepared smooth and dense TiO_2 coatings on conductors by plasma spraying. The positive DC corona test demonstrates that under the catalysis of ultraviolet light or in the electric field of the DC circuit (typically about 20 kV/cm), the TiO_2 coating will generate many electron-hole pairs, which can promote to decompose the contamination on the surface of the DC transmission line. Figure 5 demonstrates that following UV irradiation, the surface salt deposit density (S_a) of the conductor coated with TiO_2 reduced. The rectangular box in Figure 5 demonstrates that the use of TiO_2 coating can increase the corona inception voltage.

High dielectric constant and high conductivity coatings can reduce the electric field on the surface of the conductor and improve the corona discharge problem. Megala and Sugumaran (2019), Megala and Pugazhendhi Sugumaran (2020) prepared 2 mm thick polyimide/multiwalled carbon nanotubes (PI/MWCNT) coatings on ACSR. The AC corona test revealed that the surface electric field strength of the ASCR coated with 10 wt% MWCNTs was reduced by 23% compared to the bare ASCR, the AC corona inception voltage was increased by 25.87%, and the AC corona loss at 25 kV/cm was decreased by 23.53%, and the radio interference voltage (RIV) was reduced by 18 dB.

In summary, there are completely different solutions to utilize functional coatings to solve the problem of conductors corona, and which solution is optimal still needs to further investigation. Unfortunately, there has been no report on the large-scale application of anti-corona coatings, because the existing anti-corona coatings have some defects that cannot be ignored. For example, certain research has indicated that the durability of superhydrophobic coatings under corona discharge circumstances is a cause for concern. Among them, Lian et al. (2019) coated aluminum plates with the SiO_2/stearic acid superhydrophobic coating, the SCA was 169° and the sliding angle was 3°. The samples were subjected to thermal aging, corona aging, ultraviolet radiation aging, and outdoor environmental exposure tests. The test results show that high temperature and corona discharge have a strong degradation effect on the superhydrophobicity of the coating; UV and outdoor exposure age the coating, and the sliding angle increases significantly. In conclusion, the durability of the SiO_2/stearic acid superhydrophobic coating must be enhanced, and it is difficult to apply it on a large scale to overhead transmission lines.

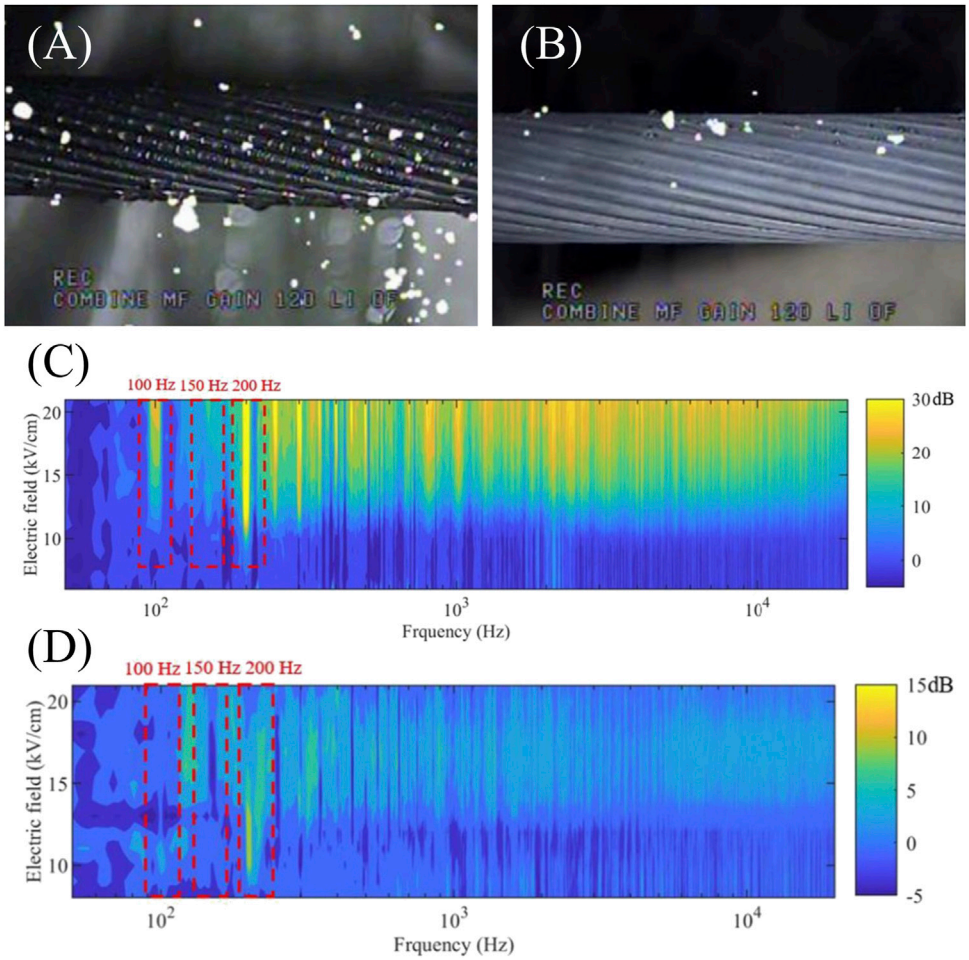

FIGURE 4
The images captured by the UV camera of **(A)** uncoated conductors, **(B)** coated conductors (Zhang et al., 2022). Measured noise levels (dB above background) as a function of electric field and frequency with continuous water spray on **(C)** uncoated conductors, **(D)** coated conductors (Zhang et al., 2022).

2.3 Coatings aim at conductors corrosion

Aluminum conductor steel reinforced (ACSR) is the most commonly used overhead conductor. However in certain hard natural environments, significant corrosion will occur and the service life will be drastically reduced, even less than 5 years in extreme cases (Li et al., 2020b). In ACSR, the aluminum line and the galvanized steel core are in direct contact, and this structure is very prone to galvanic corrosion (Håkansson et al., 2015), which is also the main form of ACSR corrosion. At the same time, mechanical wear also accelerates ASCR corrosion, and the fretting wear caused by the aeolian vibration and galloping of the conductor will lead to plastic deformation, wear, and cracking, and eventually fatigue failure (Ma et al., 2017). For transmission lines operating in coastal areas, the combined effects of salt spray corrosion and fretting wear can increase the severity of ASCR corrosion.

The anti-corrosion strategies of overhead lines include physical isolation and replacement of conductor materials. Physical isolation comprises application of anti-corrosion grease, RTV coating on the outer surface of the line, etc. ACSR coated with anti-corrosion grease has been used on a large scale, and IEC 61394:2011 has given detailed standards for anti-corrosion grease for overhead lines. In IEC 61089:1991, according to the different anti-corrosion grease coating positions, it can be divided into light anti-corrosion stranded line (only the steel core is coated with grease), medium anti-corrosion stranded line (all lines except outer layer are greased) and heavy anti-corrosion stranded line (including the outer layer all lines are greased).

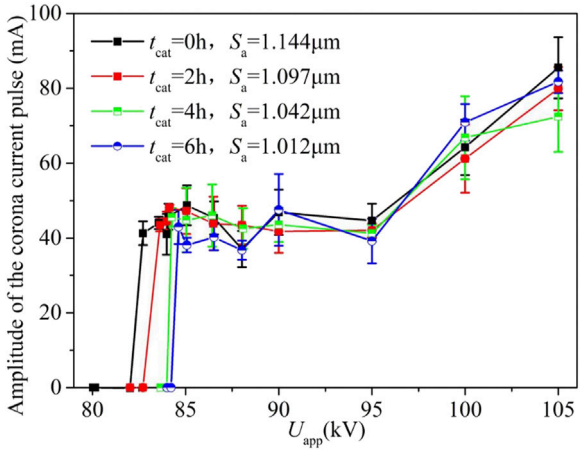

FIGURE 5
The amplitude of corona current pulse of corona current measurement results (Xu et al., 2022).

Replacing the line material refers to replacing the wire core material or core coating material, such as using aluminum conductor composite core (ACCC), aluminium clad steel reinforced (ACSR/AW) and other lines with enhanced corrosion resistance. The core in ACCC is a unidirectional carbon fiber/epoxy composite rather than galvanized steel wire in ACSR, hence galvanic corrosion will not occur for ACCC unless its glass fiber composite barrier is broken. Even if the barrier is severely broken and galvanic corrosion occurs, the galvanic corrosion rate of ACCC is much lower than that of ACSR (Håkansson et al., 2015). At the same time, ACCC also has the advantages of high-temperature low-sag (HTLS), high electrical conductivity, large bearing capacity, and light weight (Zhang et al., 2016). However, ACCC is weak in withstanding ice load and is not recommended for use in regions with extensive ice damage (Ujah et al., 2022). For replacement of core coating material, Li Q. et al. (2020) compared the corrosion resistance of ordinary galvanized steel line and Zn-5% A1-Re alloy coated steel line. After 1,000 h of neutral salt spray corrosion, the galvanized layer of galvanized steel line almost disappeared. The Zn-5% A1-Re alloy coated steel line only corroded the surface layer, and the transition layer was not corroded.

Although ASCR with anti-corrosion grease has played a certain role, there are still studies indicating that in some unique environments, such as transmission lines near factories that emit acid fumes, the use of anti-corrosion grease is not enough to prevent corrosion (Isozaki et al., 2008). In addition to coating with anti-corrosion grease, the development and application of other anti-corrosion coatings are rarely reported. It seems that the development of novel high-corrosion lines appears to be the emphasis of conductor corrosion research.

3 Coating of insulators

3.1 Coatings aim at insulators contamination

Due to human activities like industry, agriculture, transportation, and the natural environment. There is a large amount of gas, liquid, and solid contamination in the transmission line corridor (Swift et al., 2000). These contaminations may be deposited on the overhead transmission lines, and the contaminations adhere to the insulators will increase the probability of pollution flashover of the insulators, therefore seriously impact the stable operation of the transmission lines. The frequent occurrence of pollution flashover will cause the transmission line to have to be operated at a reduced voltage (Cherney, 1995; Yuan et al., 2022), resulting in a loss of transmission capacity. Coating ceramic and glass insulators with room temperature vulcanized silicon (RTV) rubber anti-pollution flashover coatings and using high temperature vulcanized silicon (HTV) composite insulators are effective methods to enhance the pollution flashover performance. Since the introduction of commercial RTV anti-pollution flashover coatings in 1978, RTV-coated insulators have been widely used (Cherney, 1995). However, field applications demonstrate that the service life of RTV is unsatisfactory (George et al., 2014), and problems such as poor coating adhesion, loss of hydrophobicity, and poor weather resistance can result in a significant deterioration in anti-pollution flashover performance. Therefore, improving the service life of RTV coatings and creating novel anti-pollution flashover coatings are the current research priorities.

The pollution flashover process on hydrophilic surfaces of ceramic and glass insulators is as follows. The contamination layer on the surface of the insulator is wet, and a dry region is formed under the heating of the leakage current. Since the conductivity of the dry region is much lower than that of the wet contamination layer, when the electric field strength on the dry region is high enough, a local arc will be generated, bridging the dry area. The local arc continues to develop along the surface of the insulator, eventually bridging the surface of the insulator and developing to a complete flashover (Nasser, 1972; Jin et al., 2022). The pollution flashover process of the hydrophobic surfaces of RTV-coated insulators and composite insulators is different from hydrophilic surfaces. There will be many small water droplets on the hydrophobic surface. The small water droplets will gradually merge into large water droplets under the action of the electric field. Partial discharges will occur at both ends of the belt, resulting in a temporary loss of hydrophobicity and the appearance of wet areas. Ultimately, the combined action of water zone growth and wet zone expansion leads to the occurrence of flashovers (Pylarinos et al., 2015; Meng et al., 2022). Although the pollution flashover processes of hydrophilic

TABLE 3 Performance comparison of typical researches about functional coatings of Insulators Contamination.

Type	Wettability [static contact Angle (SCA) and sliding angle (SA)]	Anti-pollution flashover performance (self-cleaning performace, flashover voltage, leakage current, etc.)	Durability (result of Sandpaper Abrasion test, inclined plane test, etc. tests)	References
Superhydrophobic coatings	SCA >155°, SA < 5°	Sand and dust washed away easily	After 200 g 5 m sandpaper abrasion, SCA ~150°	Peng et al. (2019)
	SCA 152°	DC flashover voltage increased by 54%	After 200 g 8 m 1,500 cW sandpaper abrasion, SCA >145°	Zhu et al. (2021)
Nonlinear coatings	SCA ~101°	Surface current of the coated insulator is much lower than the uncoated one	—	Ibrahim et al. (2014)
Sliips	SCA ~112°, SA < 7° (SCA ~71°, SA < 5° for oil droplets)	NaCl, $CuCl_2$, SiO_2, and graphite particles can remove with 50 μL water droplet	4.5 kV inclined plane test, failed after 6 h	Olad et al. (2021)
TiO2 coatings	Photoinduced superhydrophilic, under UV irradiation SCA <10°	AC flashover voltage increased by 12.8%, and the leakage current is decreased by 23.8%	—	Castaño et al. (2014)

and hydrophobic surfaces are slightly different, studies have shown that by reducing surface contamination, preventing surface wetting, and homogenizing the surface electric field are effective methods to improve the pollution flashover performance of ceramics, glass, and composite insulators.

Lastly, the performance comparison of some typical functional coatings aim at conductors icing are shown in Table 3.

3.1.1 Superhydrophobic coatings

Coating insulators with superhydrophobic coatings can prevent the surface of the insulator wetting and reduce the accumulation of contamination on the surface, hence improving the pollution flashover performance. This is due to the superhydrophobic surface has a static contact angle of more than 150° and a sliding angle of less than 10°, which can reduce the adhesion of water droplets and prevent the surface from wetting. Under the insulator shed inclination angle, the water droplets will roll off naturally on the superhydrophobic surface, and the contamination particles will be carried away by the water droplets, or adhere to the surface of the water droplets, and then roll down together with the water droplets, reducing the accumulation of contamination (Bhushan et al., 2009). This phenomenon is called self-cleaning of superhydrophobic surfaces.

Drawing on the classification method of Ghunem et al. (2022), the primary methods to produce superhydrophobic insulators are the replication molding method (Maghsoudi et al., 2018; Peng et al., 2018; Wang G. et al., 2021), etching technique (Vazirinasab et al., 2019; Patil et al., 2021), and using superhydrophobic coatings (Zhu et al., 2021).

The replication molding method makes use of the plasticity of high temperature vulcanized silicone rubber and a mold with a micro-nano structure to execute pressure vulcanization and then demoulding to obtain superhydrophobic silicone rubber. Maghsoudi et al. (2018) prepared high temperature vulcanized (HTV) silicone rubber with superhydrophobicity using the compression replication molding method with a SCA greater than 160° and a contact angle hysteresis less than 3°. Compared with the smooth HTV, the prepared superhydrophobic HTV exhibits self-cleaning ability. Wang H. et al. (2021) fabricated superhydrophobic silicone rubbers by direct replication utilizing stainless steel mesh as a template with a SCA greater than 158.5° ± 0.5° and a sliding angle of 8.9° ± 0.1°. In the self-cleaning test, contamination (carbon black) can adhere to the surface of the droplet and be carried away from the surface, which has superior self-cleaning ability compared to the smooth silicone rubber sample.

Etching technique is to use plasma treatment, laser treatment, chemical etching and other methods to process micro-nano rough structures on the substrate, so that the substrate can obtain superhydrophobicity. Vazirinasab et al. (2019) used the method of atmospheric pressure plasma treatment to directly constructe a micro-nano hierarchical superhydrophobic structure on the surface of high temperature vulcanized silicone rubber. The SCA of the prepared superhydrophobic HTV is greater than 160°. Experiments including both wet and dry contamination validated the self-cleaning characteristics of the manufactured superhydrophobic HTV. Patil et al. (2021) used a nanosecond laser to directly engrave textures on silicone rubber, giving it superhydrophobicity. The test shows that the SCA of the 50% overlapping groove structure is the largest, at 159° ± 1°, and the number of droplets required to remove contamination is the least, which corresponds to the strongest self-cleaning ability.

The superhydrophobic coating application is simpler than the first two methods. Peng et al. (2018) prepared SiO_2/epoxy superhydrophobic coatings for composite insulators using dip coating and sieve deposition methods, with a SCA greater than 155° and a sliding angle less than 5°. Even 50 abrasion cycles at a weight of 400 g, the coating's superhydrophobicity remains

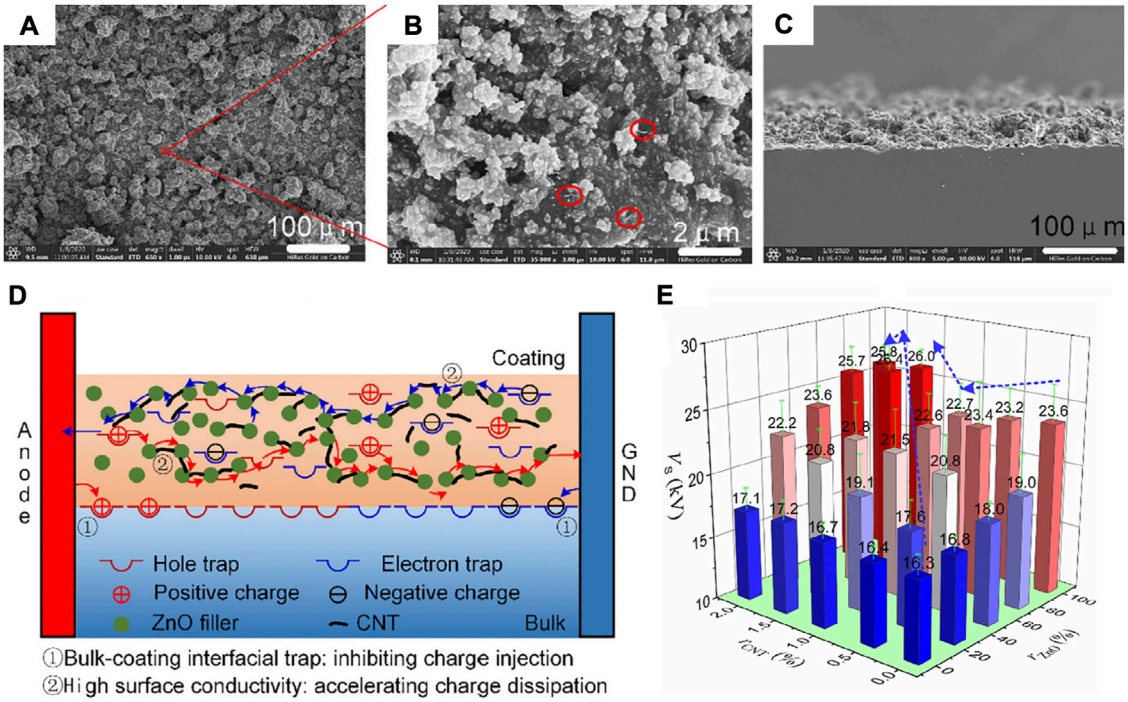

FIGURE 6
SEM images of the prepared ZnO/MWCNT/PDMS coating with **(A)** ×650 and **(B)** ×35000 magnification, The red circle is MWCNT (Zhu et al., 2021). **(C)** Cross-sectional SEM image of the coated sample (Zhu et al., 2021). **(D)** Schematic diagram describing the effect of deep interfacial traps and enhanced surface conductivity on surface charge accumulation (Zhu et al., 2021). **(E)** The flashover voltages of coating film with systematically varied concentrations of ZnO and MWCNT fillers (Zhu et al., 2021).

outstanding. In addition, the coating demonstrated remarkable anti-contamination performance, and the adhesion of dust on superhydrophobic surfaces is weak. Notably, since there is no voltage zero crossing point in high voltage direct current (HVDC) power transmission, the surface charge accumulation is more severe under DC stress, which seriously distorts the surface electric field of the insulator and promotes the occurrence of flashover (Li et al., 2020a). When designing the anti-pollution flashover coating for DC insulators, the problem of surface charge accumulation must be considered. Zhu et al. (2021) directly sprayed ZnO/MWCNT/PDMS multifunctional coatings on DC composite insulators. From the SEM images shown in Figures 6A–C, it can be seen that the coating is a uniform and dense rough surface with a micro-nano structure, and the SCA of the coating is 152°, which has superhydrophobic properties. As shown in Figure 6D, Zhu et al. established a physical model of the ZnO/MWCNT/PDMS multifunctional coating. ZnO has nonlinear conductivity, and MWCNT is a good conductor, which can form conductive channels in the coating. Under the DC electric field, conductive channels can accelerate surface charge dissipation, hence the flashover voltage can be increased. At the same time, the use of nanofillers forms many deep traps between the filler and the matrix, which can trap space charges and uniform the interfacial electric field. As shown in Figure 6E, the DC flashover test revealed that the DC pollution flashover voltage gradually rose with the addition of ZnO and MWCNT. The DC pollution flashover voltage of the coated insulator is increased by 54% in the best case. In the self-cleaning experiment, water droplets easily rolled off the superhydrophobic surface with a natural insulator inclination angle of about 5°, removing soil and sand on the surface. In conclusion, the prepared ZnO/MWCNT/PDMS coating possesses superhydrophobicity, self-cleaning, high DC surface flashover strength, good abrasion resistance, UV resistance, and anti-icing properties, and is a veritable multifunctional coating.

Although superhydrophobic coatings have demonstrated excellent self-cleaning performance in the laboratory, investigations have indicated that the coating durability issue poses a significant barrier to their widespread deployment. de Santos and Sanz-Bobi, (2021) conducted a 2-year monitoring of superhydrophobic nano-coated glass insulator strings and RTV-coated glass insulator strings in the heavily polluted area of Marseille, France. It was found that the superhydrophobic nano-coated insulator strings had superhydrophobicity only for a short time, and then gradually degraded, and the

hydrophobicity was seriously lost. However, the RTV-coated glass insulator strings exhibited lower leakage current levels and antifouling performance throughout the monitoring period. Therefore, RTV coating appears to be the best option at this stage due to its field performance and durability. Further research on superhydrophobic coatings is required to improve their durability.

3.1.2 Other coatings

Besides superhydrophobic coatings, nonlinear coatings (Ibrahim et al., 2014), Slippery Liquid Infused Porous Surfaces (SLIPS) (Olad et al., 2021), TiO_2 coatings (Zhuang, 2010; Zhuang et al., 2010; Castaño et al., 2014) have also been applied to improve the pollution flashover performance of insulators.

3.1.2.1 Nonlinear coatings

Ibrahim et al. (2014) used nanosized carbon black to adjust the I–V properties of RTV coatings and prepared nonlinear RTV coatings. AC flashover tests showed that the nonlinear coating effectively homogenizes the surface electric field and reduces the number of dry-band arcs. Meanwhile, nanosized carbon black provides conductive paths in the coating and increases the surface current, which promote the rapid drying of the wet contaminated layer. Compared to uncoated glass and ceramic insulators, the insulators coated with nonlinear coatings exhibit superior AC flashover performance in wet and contamination conditions.

3.1.2.2 Slippery liquid infused porous surfaces

Olad et al. (2021) fabricated Slippery Liquid Infused Porous Surfaces (SLIPS) on ceramic substrates by infusing a perfluorinated lubricant (Krytox 103) lubricant into 200% stretched Teflon tape. The prepared SLIPS is omniphobic, the sliding angles of water and oil are both less than 7°, and the contact angle hysteresis is less than 5°. During the self-cleaning test, the adhesion of contamination particles to SLIPS was rather low, and both common water-soluble (NaCl, $CuCl_2$) and insoluble (SiO_2, graphite) fouling particles could be easily removed from the SLIPS surface by rolling water droplets. In the inclined plane test at 4.5 kV electrical stress, SLIPS failed after 6 h, and SLIPS had outstanding electrical corrosion resistance.

3.1.2.3 TiO_2 coatings

Zhuang et al. (2010) used a sol-gel technique to prepare TiO_2 coatings on the surface of ceramic insulators. The findings of the natural pollutant deposition test indicate that the TiO_2-coated insulators exhibit enhanced self-cleaning ability in heavily polluted environments, which is because the free radicals released during the photocatalytic process of TiO_2 can decompose the contamination. Castaño et al. (2014) conducted a detailed evaluation of the electrical properties and self-cleaning properties of TiO_2-coated ceramic insulators. Compared with the untreated insulator, the AC flashover voltage of the TiO_2-coated insulator is increased by 12.8%, and the leakage current is decreased by 23.8%. The TiO_2-coated insulator remained clean after 5 months of exposure at Balsillas, whereas algae had grown on the bottom of the uncoated insulator, as shown in Figure 7. It is worth noting that, if the pollution consists primarily of inorganic particulates generated by cement plants, the self-cleaning effect of TiO_2 coating is not obvious.

Notably, the self-cleaning mechanism of the TiO_2 coating is different with the superhydrophobic coating in Section 3.1.1. First, the TiO_2 coating has photocatalytic activity, which can decompose the organic contamination attached to the surface of the insulator. Second, the TiO_2 coating is photoinduced superhydrophilic, and the SCA rapidly drops below 10° under UV irradiation. The surface of the TiO_2-coated insulator forms a continuous water film, and the settled water will be difficult to accumulate on the surface of the coating and easily flow away from the shed, hence decreasing the amount of accumulated water on the surface of the insulator. At the same time, due to the less amount of accumulated water and the large surface area of the water film, under the same conditions, the formation speed of the dry area is fast and the dry area is large, so the occurrence and development of partial discharge can be suppressed, thus reducing the occurrence of pollution flashover (Zhuang, 2010). The pollution flashover performance of the insulator was enhanced due to the combined effects of photocatalytic self-cleaning and photoinduced superhydrophilicity of the TiO_2 coatings.

Lastly, the performance comparison of typical functional coatings aim at insulators contamination are shown in Table 3.

3.2 Coatings aim at insulators icing

Icing will negatively impact the electrical performance of the insulator for two basic reasons. First, the Joule heat of the leakage current, which melts the ice and snow in some regions, making the surface of the insulator polluted and moist, and increasing the surface resistance. Second, icing will alter the shape of the insulator, especially when the icicles overlaps the shed, rapidly decreases the creepage distance (Jiang et al., 2009). Under the combined effects of contamination and icing, it is easy to cause icing flashover of insulators. Farzaneh et al. (2010) quantified the severity of insulator icing (mild, moderate, severe) and analyzed the ice flashover process under each icing level in conjunction with the icing flashover accidents in different regions. Icing flashover is a very complex process, and the conductivity of water and the shape, quantity, and distribution of ice-coated insulators have the greatest impact on the icing flashover.

Due to the insulator's unique form and high insulation pressure, the majority of anti-icing and de-icing techniques

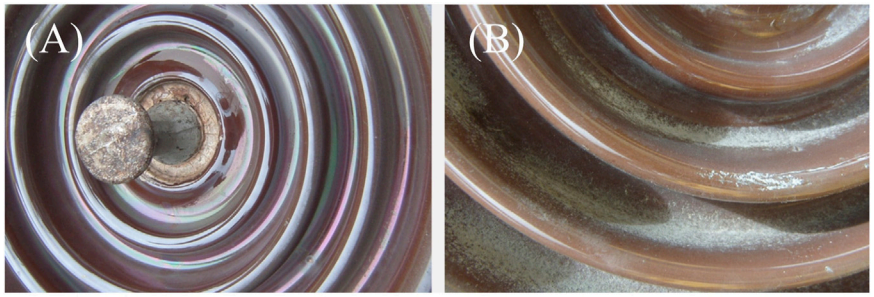

FIGURE 7
The images of **(A)** the coated TiO_2 coating and **(B)** the uncoated TiO_2 coating insulators tested in service in Balsillas during 5 months (Castaño et al., 2014).

utilized on conductors are inapplicable. Changing the layout of insulators, such as V-shaped arrangement (Pu et al., 2011; Wei et al., 2014) and alternating large and small sheds (Zhang et al., 2012) can increase the icing performance of insulators. However, the above solutions do not fundamentally solve the problem of insulator icing, but only play a mitigating role. Insulator icing solutions coated with functional coatings, such as semiconductor coatings and superhydrophobic coatings, have exhibited unique advantages.

3.2.1 Semiconductor coatings

Anti-icing by semiconductor coating refers to reducing the surface resistance of insulators by adding conductive fillers (such as carbon black, ZnO, and carbon fiber) into the coating and utilizing the Joule heat generated by leakage current for anti-icing. Liao et al. (2007) prepared semiconductor RTV coatings on ceramic insulators using carbon black as filler. The icing simulation test and icing flashover test show that, compared with the original insulator, the insulator coated with the semiconductor RTV coating does not appear icicles that overlap the shed, the ice accumulation is reduced by 50%, and the icing flashover voltage is greatly improved. Qin et al. (2009) examined the influence of RTV coatings with varying electrical conductivities on anti-icing performance. Experiments indicate that the heat generated by the leakage current in the dry region at the shed's edge will render the icicle's root unstable, resulting in its will easily fall off by natural forces. The leakage current of XP-70 insulator coated with semiconductor RTV coating can reach 5–20 mA, and the anti-icing effect can be adjusted by changing the conductivity of the coating. The higher conductivity of the coating, the larger the leakage current, the more heat generated, and the better the anti-icing effect. Wei et al. (2012) applied a semiconductor RTV coating only on the bottom of the insulator in order to reduce the power loss caused by the continuous leakage current. In this way, only when the water film or ice layer bridges the upper surface of the insulator, a conductive path will be formed. Under normal conditions, the power loss is very low. However, this coating method is only effective for glaze, but not for soft rime, and is very sensitive to the conductivity of water film and ice layer. Wei et al. (2016) improved the coating method of semiconductor coatings again. The test results show that the surface resistance of the coating should be less than 0.3 MΩ. It is a better choice to apply the semiconductor coating on the lower surface and the outer edge of the upper surface of the insulator with a 5–8 cm exposed area. Li et al. (2016) and Yan et al. (2016) prepared carbon/nano-silica/PDMS coatings with both semiconducting and superhydrophobic properties on insulators via dip coating and self-assembly techniques. The SEM image is shown in Figure 8A. The SCA of the coating is 155° and the sliding angle is less than 8°. In the icing simulation test at −6°C and 12 kV AC, the average leakage current of the carbon/nano-silica/PDMS coated insulator is 9.8 mA, the leakage current waveform is shown in Figure 8B. The average surface temperature of the coated insulator is 3°C, and the amount of ice is significantly less than that of the uncoated insulator. The thermal infrared images of 1.5 h are shown in Figures 8C,D. The coated insulator has a 50% higher icing flashover voltage than the uncoated insulator.

There are two obvious defects with the use of semiconductor coatings for insulator anti-icing: one is large power loss; the other is due to the high leakage current flowing in the coating under working conditions, which will cause the coating to age (Wei et al., 2016). The problem of power loss is somewhat resolved by the partial coating method. However, there are few studies on the aging problem of semiconductor coatings during long-term operation. The durability of semiconductor coatings should be investigated further.

3.2.2 Superhydrophobic coatings

The anti-icing mechanism of superhydrophobic surfaces is briefly introduced in Section 2.1.1. Similarly, superhydrophobic coatings are also suitable for anti-icing on insulators. Li et al. (2014) prepared SiO_2 micro-nano

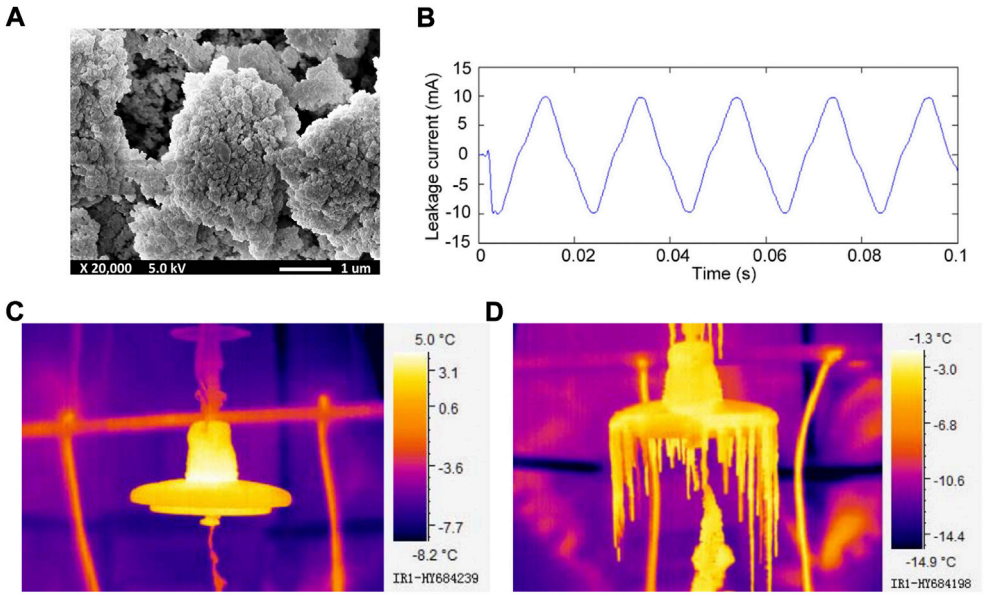

FIGURE 8
(A) The SEM image of the carbon/nano-silica/PDMS coating (Li et al., 2016). **(B)** Typical leakage current waveforms of insulators with carbon/nano-silica/PDMS coating (Yan et al., 2016). Thermal infrared images of tested insulators after 1.5 h energized icing: **(C)** the insulator with the carbon/nano-silica/PDMS coating; **(D)** uncoated glass insulator (Yan et al., 2016).

hierarchical rough structure via sol-gel method and used fluorosilane for low surface energy modification, and successfully produced superhydrophobic coatings on the surface of glass insulators with SCA of 163.6° and sliding angle 1.4°. Excellent anti-icing and anti-fog performance were demonstrated in outdoor snow accumulation test and test hanging on a tower. Guo et al. (2015) fabricated a $CaCO_3$/SiO_2/fluorosilicone/epoxy superhydrophobic coating on glass insulators utilizing nanoparticle filling and hot water etching method. The SCA was 166.4° and the sliding angle was less than 1°. In the glaze icing test, the water droplets bounced off and slid off the superhydrophobic insulator, resulting in the ice accumulation is greatly reduced compared to the uncoated insulator. Zuo et al. (2015) fabricated a nano-SiO_2/fluorosilicone/epoxy superhydrophobic coating on glass insulators by direct spraying. The SCA was 161.1° and the sliding angle was less than 1°. In the glaze ice simulation test, compared with the original insulator, the AC icing flashover voltage was increased by 27%. Emelyanenko et al. (2017) utilized nanosecond laser treatment to construct a rough texture on the surface of silicone rubber, the SEM images are shown in Figures 9A,B, and then grafted a layer of fluorosilane molecules to create a superhydrophobic surface. The SCA was 170°. In the outdoor ice accretion test, the superhydrophobic silicone rubber can effectively prevent the accumulation of ice at 0°C, as shown in Figure 9C. Figure 9D demonstrates that at −17°C, the amount of snow accumulation is drastically reduced compared to the untreated silicone rubber. Sun et al. (2020) used the sol-gel method combined with a plasma treatment method to prepare a superhydrophobic surface on the silicone rubber. The SCA was 160.15° and the sliding angle was 1.8°. In the freezing test at −30°C, the freezing time of water droplets on the surface of the superhydrophobic silicone rubber was delayed by 6 times compared to the untreated silicone rubber. Hong et al. (2022) used Femtosecond laser treatment and PDMS modification to prepare superhydrophobic alumina ceramics with a SCA of 176.39° and a sliding angle of 1°. Compared with the untreated ceramic, the solidification time is delayed by 189 s.

It is worth noting that related studies have suggested that superhydrophobicity seems to be necessary, and the hydrophobic surface will decrease the icing flashover performance of the insulator. Jiang et al. (2010) noted that RTV coatings are only effective for short-term icing. In the short-time icing conditions, due to the hydrophobicity of the RTV coating, the development of ice was delayed, but the icing was still formed, and the icing was granular and formed tiny voids in the ice layer. In severe icing conditions, since there are numerous voids between the RTV coating surface and the ice surface, it is more likely to generate partial discharge and melt the ice layer, resulting in a high leakage current. At the same time, partial discharge will also damage the RTV coating. For the above reasons, RTV-coated insulators have lower icing flashover voltage in severe icing conditions.

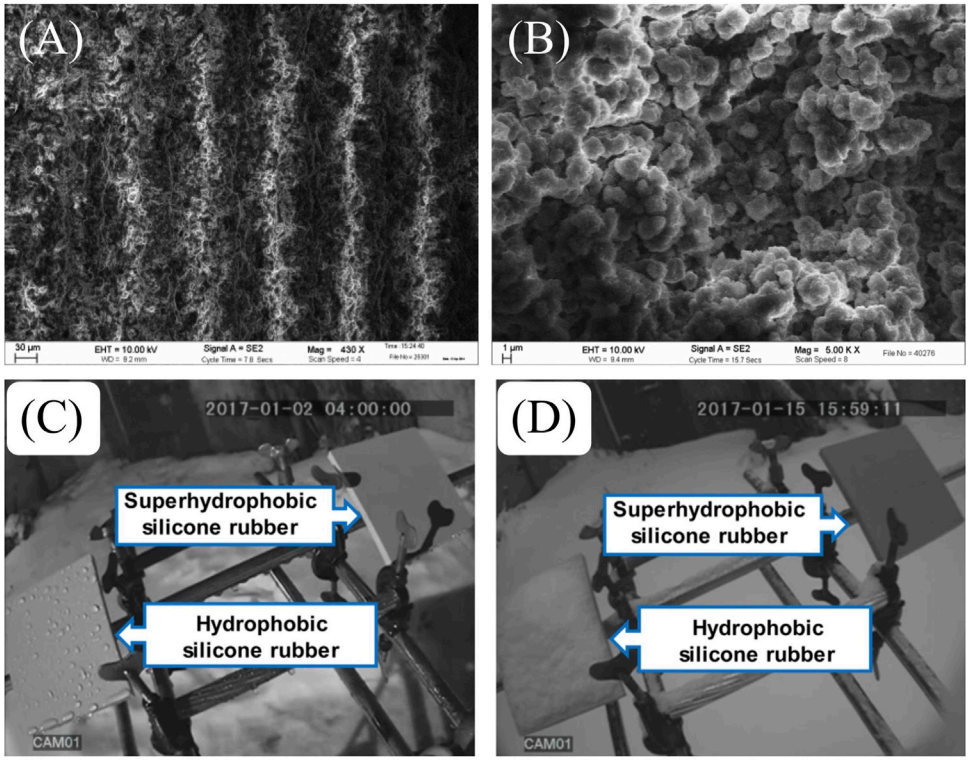

FIGURE 9
The SEM images of the laser-textured surface of silicone rubber at **(A)** 30 μm and **(B)** 1 μm (Emelyanenko et al., 2017). Behavior of hydrophobic silicone rubber and superhydrophobic silicone rubber during rain **(C)** and during snow **(D)** (Emelyanenko et al., 2017).

3.2.3 Other coatings

In addition to semiconductor coatings and superhydrophobic coatings, anti-icing coatings of insulators with phase change materials (Hu et al., 2021; Yuan et al., 2021) and Slippery Liquid Infused Porous Surfaces (Zhu et al., 2013) also were developed.

3.2.3.1 Coatings with phase change materials

Hu et al. (2021) prepared MPCM/RTV anti-icing coatings by mixing room temperature vulcanized (RTV) silicone rubber and phase change microcapsules (MPCM). MPCM with SiO_2 shell and n-tetradecane core was fabricated by *in-situ* polymerization method with the freezing temperature of 2.3°C and the latent heat of 130.8 J/g. At −10°C, the prepared anti-icing coating can be kept above 0°C for approximately 6 min. Yuan et al. (2021) prepared MPCM/PRTV anti-icing coatings by modifying permanent room temperature vulcanized (PRTV) silicone rubber using phase change microcapsules (MPCM). MPCM uses MUF resin as the shell and n-tetradecane as the core. The addition of MPCM roughens the coating's surface, allowing it to develop superhydrophobic characteristics with the SCA of 164°and the sliding angle of 6°. In the -5°C freezing test, the freezing time of water droplets on the prepared MPCM/PRTV coating was 1.48 times longer than that of the PRTV coating. The freezing and process comparison images are shown in Figures 10A,B. At the same time, the adhesion of ice is reduced by 15%. After 15 icing/deicing cycles, the SCA of the MPCM/PRTV coating still remains above 160°. Figures 10C,D show SEM images demonstrating that the coating remains intact and that the MPCM is not cracked. It can be seen that the coating has good durability.

3.2.3.2 Slippery liquid infused porous surfaces

Zhu et al. (2013) prepared silicone oil infused polydimethylsiloxane (PDMS) SLIPS coating on the glass insulator with a SCA of 115°. The results of the tests indicate that the adhesion of ice to the SLIPS coating is only 50 kPa, and the ice can only form a loose ice layer on the SLIPS insulator, which can easily fall off under the action of natural forces.

4 Coating of towers

Transmission line towers are primarily composed of galvanized steel. The presence of moisture, salt, acid gases, etc.

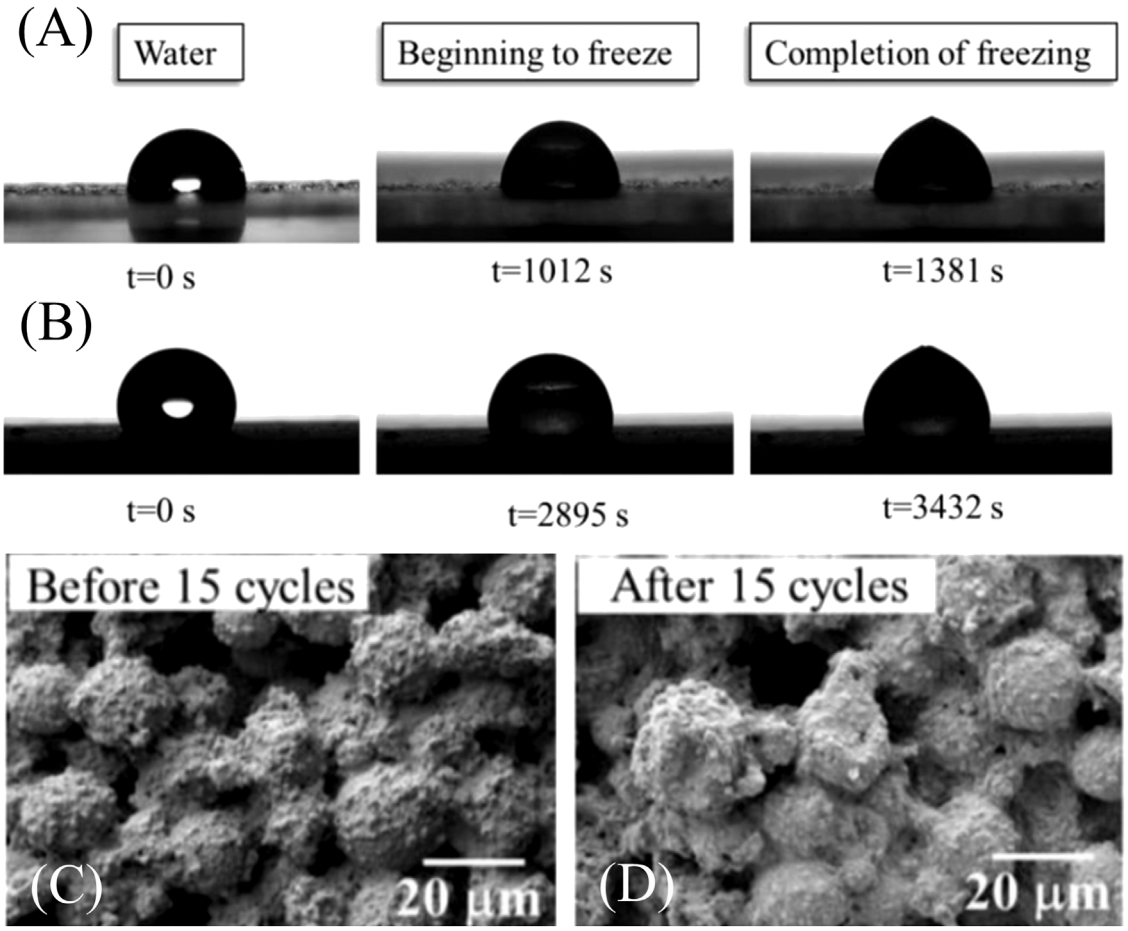

FIGURE 10
Freezing time of water droplet on **(A)** PRTV and **(B)** MPCM/PRTV coatings (Yuan et al., 2021). The SEM images of MPCM/PRTV coating **(C)** before 15 icing/melting cycles and **(D)** after (Yuan et al., 2021).

in the environment will hasten the deterioration of the galvanized layer, resulting in rust and corrosion. Therefore, the tower needs anti-corrosion coatings for protection. In ISO 9223:2012, atmospheric corrosiveness is classified into six categories: C1 ~ C5 and CX. Among them, the typical environmental cases of C3 are urban and industrial atmospheres, moderate sulfur dioxide pollution areas and low salinity coastal areas. The typical environmental cases of C4 are industrial areas and coastal areas with moderate salinity. The typical environmental cases of C5 are industrial areas with harsh atmospheres, coastal and offshore areas with high salinity and humidity. The primer-intermediate-topcoat three-layer coating system should be utilized for towers in air corrosion environments C3–C5.

Due to the zinc metal layer on the surface of the tower, ISO 12944-5:2018 points that should utilize epoxy coatings rather than alkyd coatings as primers. Zinc-rich primers (Knudsen et al., 2005; Shreepathi et al., 2010; Xu et al., 2019; Hussain et al., 2021) and zinc phosphate primers (Shao et al., 2009; Hao et al., 2013; Alibakhshi et al., 2014) are more commonly used. Epoxy micaceous iron oxide intermediate is the most common intermediate (Nikravesh et al., 2011; Arman et al., 2013). Acrylic topcoats (Ecco et al., 2016) are the most commonly used topcoats, while epoxy coatings are unsuitable. It is important to note that anti-corrosion paint should not drip onto the insulator during on-site construction. Wang et al. (2016) discovered that if the anti-corrosion paint (composed of zinc-rich epoxy primer, epoxy micaceous iron oxide intermediate, and acrylate topcoat) drips on the composite insulator surface, the electrical performance of the insulator will be degraded. The test findings indicate that the anti-corrosion coating will reduce the hydrophobicity and hydrophobic recovery ability of the composite insulator. The larger the area of the anti-corrosion coating, the lower the pollution flashover voltage.

In recent years, researchers have also been developing new types of plating and anti-corrosion coatings. Popoola et al. (2016)

prepared a Zinc-Yttria electroplating bath for electroplating. The experimental results show that the addition of yttrium oxide particles in the electroplating process improves the corrosion behavior of the steel plate in NaCl solution. The addition of Yttria helps create a dense structure in the plating, which improves corrosion and wear resistance. Fan et al. (2020) prepared CeO_2-polyaniline conductive capsules using *in-situ* chemical oxidation polymerization. The capsules were dispersed in epoxy resin and then sprayed on the surface of steel plate to form an anti-corrosion coating. The experimental structures show that the coatings containing CeO_2-polyaniline capsules exhibit excellent corrosion resistance with an impedance modulus higher than $10^9\ \Omega\ cm^2$, which is 10 times higher than that of conventional PANI-Epoxy coatings. Lv et al. (2021) prepared Zn/PMHS (Polymethylhydrogensiloxane) superhydrophobic coatings on steel plates using sandpaper grinding and low surface energy modification. The test findings indicate that the drag reduction rate for the prepared superhydrophobic coating is 45%. The superhydrophobicity can be maintained for a long time in 3.5% NaCl solution, hence extending the cathodic protection time of zinc powder. Nayak et al. (2021) used f-MWCNT/PIn (functionalized multi-walled carbon nanotube/polyindole) nanocomposites to prepare epoxy resin coatings with superior corrosion resistance. The experimental results demonstrate that the 0.25 wt% f-MWCNT/PIn blended nanocomposite coating possesses excellent anti-corrosion and barrier protection properties. Wang G. et al. (2021) prepared a CeO_2-Polyurethane anti-corrosion coating with near infrared activated self-healing capability. The mechanical characteristics and corrosion resistance are unchanged after the coating self-healed. The low-frequency impedance modulus of the CeO_2-Polyurethane anti-corrosion coating reaches $1.29 \times 10^9\ \Omega\ cm^2$, indicating outstanding anti-corrosion performance.

In addition to the corrosion problem, the tower also needs to face the problem of icing. However, in Section 2.1, the anti-icing coating of the conductors (developed on the aluminum substrate) has been introduced in detail, and the development of anti-icing coatings on galvanized steel and aluminum shows great similarity. Therefore, it will not be repeated here.

5 Conclusion and outlook

This paper reviews the status of the current application and the performance mechanism of functional coating for overhead transmission lines. Coatings with properties such as superhydrophobicity, self-cleaning, photocatalysis, semiconduction, and anti-corrosion have demonstrated obvious advantages in solving problems such as conductor icing, corona, and corrosion; insulator contamination and icing; tower corrosion. Functional coatings provide low cost, high efficiency, low energy consumption, and light weight solutions, and have the potential for large-scale application.

However, there are still a few crucial difficulties that need to be further studied. There are three primary issues in the study of functional coating for overhead transmission lines:

1) Investigate the feasibility of the preparation method of functional coatings applied to the electrical equipment. During the initial test stage of functional coatings development, tests are often conducted on aluminum sheets, glass sheets, ceramic sheets, and other substrates that are the same as those of electrical equipment. Due to the complex shape, large surface area, and complex operation conditions of the real electrical equipment, it is necessary to carry out tests on conductors, insulators, and towers in operation. While verifying the feasibility of the preparation method on the electrical equipment, the real performance of the functional coating under the superposition of various stresses can also be investigated. For example, in the process of using silane to modify the hydrophobicity and low surface energy, there are complications such as method complicated, time consuming, and expensive. Whether it can be successfully applied to hundreds of kilometers of ACSR remains to be studied. Another example, real glass insulators are different from flat glass sheets. Whether the preparation method can uniformly coat the surface of the insulator needs to be verified by experiments.
2) Strengthen the research on the durability of functional coatings. In almost all conditions, durability is a crucial factor in determining whether a coating can be large-scale applied. The operating environment of overhead transmission lines is complicated. Icing, deicing, ultraviolet radiation, salt spray corrosion, corona discharge, and mechanical friction, etc., are all huge challenges for the durability of coatings. For example, the superhydrophobic properties of superhydrophobic coatings are highly dependent on the surface micro-nano structure and surface chemical properties. Under the influence of mechanical wear and corona discharge, the superhydrophobic properties will seriously degrade and may be irreversibly destroyed. Therefore, when developing functional coatings for transmission lines, it is necessary to strengthen the durability design. At the same time, it is recommended to conduct long-term monitoring of coating performance under operating conditions to evaluate its durability.
3) Focus on the development of composite functional coatings. The problems of overhead transmission lines are diverse and complex, such as conductor icing and conductor corona, which may occur simultaneously, and a single functional coating may not be enough to meet the requirements. As the understanding of transmission line problem mechanisms deepen, connections between the

problems may be revealed, and thus the development of composite functional coatings can be attempted.

In summary, with the continuous progress of the preparation method, the gradual improvement of coating durability, and the in-depth research on the mechanism of transmission line problems, functional coatings are expected to become the first choice for solving overhead transmission line problems.

Author contributions

BT: Writing-original draft, Conceptualization, Methodology. LC: Resources, Supervision, Writing-review and editing. JW: Writing, Investigation. XZ: Supervision, Investigation. RL: Supervision, Funding acquisition.

Funding

This work was supported by the National Natural Science Foundation of China (Grant No. 52077013).

Acknowledgments

Thanks for the strong guidance given by LC in the writing of the paper, the help of JW and XZ, and the financial support of RL.

Conflict of interest

The authors declare that the research was conducted in the absence of any commercial or financial relationships that could be construed as a potential conflict of interest.

Publisher's note

All claims expressed in this article are solely those of the authors and do not necessarily represent those of their affiliated organizations, or those of the publisher, the editors and the reviewers. Any product that may be evaluated in this article, or claim that may be made by its manufacturer, is not guaranteed or endorsed by the publisher.

References

Alibakhshi, E., Ghasemi, E., and Mahdavian, M. (2014). Sodium zinc phosphate as a corrosion inhibitive pigment. *Prog. Org. Coatings* 77, 1155–1162. doi:10.1016/j.porgcoat.2014.03.027

Arman, S. Y., Ramezanzadeh, B., Farghadani, S., Mehdipour, M., and Rajabi, A. (2013). Application of the electrochemical noise to investigate the corrosion resistance of an epoxy zinc-rich coating loaded with lamellar aluminum and micaceous iron oxide particles. *Corros. Sci.* 77, 118–127. doi:10.1016/j.corsci.2013.07.034

Bhushan, B., Jung, Y. C., and Koch, K. (2009). Self-cleaning efficiency of artificial superhydrophobic surfaces. *Langmuir* 25, 3240–3248. doi:10.1021/la803860d

Bian, X., Li, H., Zhang, X., Cui, X., Lu, T., and Song, W. (2018). Influence of fine particulate matter on the variation of surface morphologies of conductors subjected to positive DC voltages. *Appl. Phys. Lett.* 113, 204102. doi:10.1063/1.5044389

Bian, X., Lin, Y., Pi, X., Lu, T., Xu, F., Li, H., et al. (2019). Corona characteristics of conductor with TiO2 hydrophilic film subjected to DC high voltage. *J. Eng. (Stevenage).* 2019, 3046–3050. doi:10.1049/joe.2018.8424

Boinovich, L. B., and Emelyanenko, A. M. (2013). Anti-icing potential of superhydrophobic coatings. *Mendeleev Commun.* 1, 3–10. doi:10.1016/j.mencom.2013.01.002

Boinovich, L. B., Emelyanenko, A. M., Emelyanenko, K. A., and Modin, E. B. (2019). Modus operandi of protective and anti-icing mechanisms underlying the design of longstanding outdoor icephobic coatings. *ACS Nano* 13, 4335–4346. doi:10.1021/acsnano.8b09549

Cao, Y., Lu, Y., Liu, N., Li, Y., Wang, P., Dai, C., et al. (2022). Multi-applicable, durable superhydrophobic anti-icing coating through template-method and chemical vapor deposition. *Surfaces Interfaces* 32, 102100. doi:10.1016/j.surfin.2022.102100

Castaño, J. G., Velilla, E., Correa, L., Gómez, M., and Echeverría, F. (2014). Ceramic insulators coated with titanium dioxide films: Properties and self-cleaning performance. *Electr. Power Syst. Res.* 116, 182–186. doi:10.1016/j.epsr.2014.06.009

Cherney, E. A. (1995). RTV silicone-a high tech solution for a dirty insulator problem. *IEEE Electr. Insul. Mag.* 11, 8–14. doi:10.1109/57.475903

de Santos, H., and Sanz-Bobi, M. Á. (2021). Research on the pollution performance and degradation of superhydrophobic nano-coatings for toughened glass insulators. *Electr. Power Syst. Res.* 191, 106863. doi:10.1016/j.epsr.2020.106863

Ecco, L. G., Fedel, M., Deflorian, F., Becker, J., Iversen, B. B., and Mamakhel, A. (2016). Waterborne acrylic paint system based on nanoceria for corrosion protection of steel. *Prog. Org. Coatings* 96, 19–25. doi:10.1016/j.porgcoat.2016.02.010

Emelyanenko, A. M., Boinovich, L. B., Bezdomnikov, A. A., Chulkova, E. V., and Emelyanenko, K. A. (2017). Reinforced superhydrophobic coating on silicone rubber for longstanding anti-icing performance in severe conditions. *ACS Appl. Mat. Interfaces* 9, 24210–24219. doi:10.1021/acsami.7b05549

M. Farzaneh, H. Gauthier, G. Castellana, C. Engelbrecht, Á. J. ELÍASSON, S. M. Fikke, et al. (2015). *Coatings for protecting overhead power network equipment in winter conditions: Working Group B2* (Paris: CIGRÉ), 44.

Fan, W., Wang, H., Wang, C., Liu, Z., Zhu, Y., and Li, K. (2020). Epoxy coating capable of providing multi-component passive film for long-term anti-corrosion of steel. *Appl. Surf. Sci.* 521, 146417. doi:10.1016/j.apsusc.2020.146417

Farzaneh, M., Jakl, F., Arabani, M. P., Elíasson, Á., Fikke, S., Gallego, A., et al. (2010). *Systems for prediction and monitoring of ice shedding, anti-icing and de-icing for power line conductors and ground wires*. Paris: CIGRÉ.

Farzaneh, M., Volat, C., and Leblond, A. (2008). "Anti-icing and de-icing techniques for overhead lines," in *Atmospheric icing of power networks*. Editor M. Farzaneh (Dordrecht: Springer Netherlands), 229–268. doi:10.1007/978-1-4020-8531-4_6

Fenero, M., Knez, M., Saric, I., Petravic, M., Grande, H., and Palenzuela, J. (2020). Omniphobic etched aluminum surfaces with anti-icing ability. *Langmuir* 36, 10916–10922. doi:10.1021/acs.langmuir.0c01324

George, J. -M., Prat, S., Lumb, C., Virlogeux, F., Gutman, I., Lundengård, J., et al. (2014). Field experience and laboratory investigation of glass insulators having a factory-applied silicone rubber coating. *IEEE Trans. Dielectr. Electr. Insul.* 21, 2594–2601. doi:10.1109/TDEI.2014.004600

Ghunem, R. A., Cherney, E. A., Farzaneh, M., Momen, G., Illias, H. A., Mier, G., et al. (2022). Development and application of superhydrophobic outdoor insulation: A review. *IEEE Trans. Dielectr. Electr. Insul.* 29, 1392–1399. doi:10.1109/TDEI.2022.3183671

Guarnieri, M. (2013). The beginning of electric energy transmission: Part One [historical]. *EEE. Ind. Electron. Mag.* 7, 50–52. doi:10.1109/MIE.2012.2236484

Guo, C., Liao, R., Yuan, Y., Zuo, Z., and Zhuang, A. (2015). Glaze icing on superhydrophobic coating prepared by nanoparticles filling combined with etching method for insulators. *J. Nanomater.* 2015, e404071–7. doi:10.1155/2015/404071

Håkansson, E., Predecki, P., and Kumosa, M. S. (2015). Galvanic corrosion of high temperature low sag aluminum conductor composite core and conventional aluminum conductor steel reinforced overhead high voltage conductors. *IEEE Trans. Reliab.* 64, 928–934. doi:10.1109/TR.2015.2427894

Hao, Y., Liu, F., Han, E.-H., Anjum, S., and Xu, G. (2013). The mechanism of inhibition by zinc phosphate in an epoxy coating. *Corros. Sci.* 69, 77–86. doi:10.1016/j.corsci.2012.11.025

Hong, Z., Wang, W., Ma, Z., Lu, M., Pan, S., Shi, E., et al. (2022). Anti-icing ceramics surface induced by femtosecond laser. *Ceram. Int.* 48, 10236–10243. doi:10.1016/j.ceramint.2021.12.238

Hu, Q., Deng, Y., Xiao, L., Shu, L., Jiang, X., Zhou, L., et al. (2021). Study on modification of room temperature vulcanized silicone rubber by microencapsulated phase change material. *J. Energy Storage* 41, 102842. doi:10.1016/j.est.2021.102842

Hussain, A. K., Seetharamaiah, N., Pichumani, M., and Chakra, Ch. S. (2021). Research progress in organic zinc rich primer coatings for cathodic protection of metals – a comprehensive review. *Prog. Org. Coatings* 153, 106040. doi:10.1016/j.porgcoat.2020.106040

Hylten-Cavallius, N., Annestrand, S., Witt, H., and Madzarevic, V. (1964). Insulation requirements, corona losses, and corona radio interference for high-voltage D-C lines. *IEEE Trans. Power Appar. Syst.* 83, 500–508. doi:10.1109/TPAS.1964.4766030

Ibrahim, M. E., Sabiha, N. A., and Izzularab, M. A. (2014). Nanofilled nonlinear coating material for improving proactive flashover performance of high voltage insulators. *IEEE Trans. Dielectr. Electr. Insul.* 21, 2156–2163. doi:10.1109/TDEI.2014.004227

Isozaki, M., Adachi, K., Hita, T., and Asano, Y. (2008). Study of corrosion resistance improvement by metallic coating for overhead transmission line conductor. *Elect. Eng. Jpn.* 163, 41–47. doi:10.1002/eej.20365

Jiang, G., Chen, L., Zhang, S., and Huang, H. (2018). Superhydrophobic SiC/CNTs coatings with photothermal deicing and passive anti-icing properties. *ACS Appl. Mat. Interfaces* 10, 36505–36511. doi:10.1021/acsami.8b11201

Jiang, X., Ma, J., Zhang, Z., and Hu, J. (2010). Effect of hydrophobicity coating on insulator icing and DC flashover performance of iced insulators. *IEEE Trans. Dielectr. Electr. Insul.* 17, 351–359. doi:10.1109/TDEI.2010.5448088

Jiang, X., Shu, L., and Sun, C. (2009). *Power system contamination and icing insulation*. Beijing: China Electric Power Press.

Jie, Z., Zichen, H., Jiale, W., and Xingming, B. (2020). Experimental studies on effects of surface morphologies on corona characteristics of conductors subjected to positive DC voltages. *High. Volt.* 5, 489–497. doi:10.1049/hve.2019.0317

Jin, H., Nie, S., Li, Z., Tong, C., and Wang, K. (2018). Investigation on preparation and anti-icing performance of super-hydrophobic surface on aluminum conductor. *Chin. J. Chem. Phys.* 31, 216–222. doi:10.1063/1674-0068/31/cjcp1707152

Jin, L., Zhou, G., Yuan, Z., Jin, H., and Man, X. (2022). Study on initial discharge process of insulator pollution flashover considering quantum. *IEEE Trans. Dielectr. Electr. Insul.*, 1. doi:10.1109/TDEI.2022.3190346

Karady, G. G., Shah, M., and Brown, R. L. (1995). Flashover mechanism of silicone rubber insulators used for outdoor insulation-I. *IEEE Trans. Power Deliv.* 10, 1965–1971. doi:10.1109/61.473356

Kim, P., Wong, T.-S., Alvarenga, J., Kreder, M. J., Adorno-Martinez, W. E., and Aizenberg, J. (2012). Liquid-infused nanostructured surfaces with extreme anti-ice and anti-frost performance. *ACS Nano* 6, 6569–6577. doi:10.1021/nn302310q

Knudsen, O. Ø., Steinsmo, U., and Bjordal, M. (2005). Zinc-rich primers—test performance and electrochemical properties. *Prog. Org. Coatings* 54, 224–229. doi:10.1016/j.porgcoat.2005.06.009

Kulinich, S. A., Farhadi, S., Nose, K., and Du, X. W. (2011). Superhydrophobic surfaces: Are they really ice-repellent? *Langmuir* 27, 25–29. doi:10.1021/la104277q

Li, B., He, J., Li, Y., and Zheng, Y. (2020a). "Chapter 1 - introduction," in *Protection technologies of ultra-high-voltage AC transmission systems*. Editors B. Li, J. He, Y. Li, and Y. Zheng (Academic Press), 1–17. doi:10.1016/B978-0-12-816205-7.00001-7

Li, B., Liu, L., Dang, P., Wang, G., Tang, L., and Li, T. (2020b). "Study on corrosion test of corrosion-proof steel core of high-anticorrosive conductor," in 2020 IEEE International Conference on High Voltage Engineering and Application (ICHVE), Beijing, China, 06-10 September 2020, 1–4. doi:10.1109/ICHVE49031.2020.9280059

Li, J., Huang, Z., Yan, X., and Wei, Y. (2016). An OH-PDMS-modified nano-silica/carbon hybrid coating for anti-icing of insulators part I: Fabrication and small-scale testing. *IEEE Trans. Dielectr. Electr. Insul.* 23, 935–942. doi:10.1109/TDEI.2015.005234

Li, Q., Naderiallaf, H., Lei, Z., Wang, Y., Liu, P., Zhang, L., et al. (2020). Surface charge pattern analysis based on the field-dependent charging theory: A review. *IEEE Trans. Dielectr. Electr. Insul.* 27, 257–269. doi:10.1109/TDEI.2019.008430

Li, X., Yang, B., Zhang, Y., Gu, G., Li, M., and Mao, L. (2014). A study on superhydrophobic coating in anti-icing of glass/porcelain insulator. *J. Solgel. Sci. Technol.* 69, 441–447. doi:10.1007/s10971-013-3243-y

Lian, C., Zhang, X., Emersic, C., Lowndes, R., and Cotton, I. (2019). "Long-term durability of stearic acid silicon dioxide nanoparticle superhydrophobic coating on aluminium alloy overhead line conductors," in 2019 IEEE Electrical Insulation Conference (EIC), 16-19 June 2019, Calgary, AB, Canada, 238–241. doi:10.1109/EIC43217.2019.9046592

Liao, R., Zuo, Z., Guo, C., Yuan, Y., and Zhuang, A. (2014). Fabrication of superhydrophobic surface on aluminum by continuous chemical etching and its anti-icing property. *Appl. Surf. Sci.* 317, 701–709. doi:10.1016/j.apsusc.2014.08.187

Liao, W., Jia, Z., Guan, Z., Wang, L., Yang, J., Fan, J., et al. (2007). Reducing ice accumulation on insulators by applying semiconducting RTV silicone coating. *IEEE Trans. Dielectr. Electr. Insul.* 14, 1446–1454. doi:10.1109/TDEI.2007.4401227

Liu, G., Yuan, Y., Jiang, Z., Youdong, J., and Liang, W. (2020a). Anti-frosting/anti-icing property of nano-ZnO superhydrophobic surface on Al alloy prepared by radio frequency magnetron sputtering. *Mat. Res. Express* 7, 026401. doi:10.1088/2053-1591/ab6e33

Liu, G., Yuan, Y., Liao, R., Wang, L., and Gao, X. (2020b). Fabrication of a porous slippery icephobic surface and effect of lubricant viscosity on anti-icing properties and durability. *Coatings* 10, 896. doi:10.3390/coatings10090896

Liu, G., Yuan, Y., Liao, R., Yu, Q., and Wang, L. (2021). "Fabrication of durable superhydrophobic aluminium surface and its anti-icing properties," in 2021 International Conference on Electrical Materials and Power Equipment (ICEMPE), Chongqing, China, 11-15 April 2021, 1–4. doi:10.1109/ICEMPE51623.2021.9509114

Liu, G. Y., Yuan, Y., Liao, R. J., Xiang, H. Y., Wang, L., Yu, Q., et al. (2022). Robust and self-healing superhydrophobic aluminum surface with excellent anti-icing performance. *Surfaces Interfaces* 28, 101588. doi:10.1016/j.surfin.2021.101588

Liu, J., Li, R., Lei, Y., Zhang, Z., and Fu, H. (2021). "Research on a passive non-interventional combined anti-icing method for overhead line structure," in 2021 International Conference on Electrical Materials and Power Equipment (ICEMPE), Chongqing, China, 11-15 April 2021, 1–4. doi:10.1109/ICEMPE51623.2021.9509178

Liu, Q., Yang, Y., Huang, M., Zhou, Y., Liu, Y., and Liang, X. (2015). Durability of a lubricant-infused Electrospray Silicon Rubber surface as an anti-icing coating. *Appl. Surf. Sci.* 346, 68–76. doi:10.1016/j.apsusc.2015.02.051

Liu, Y., Xu, R., Luo, N., Liu, Y., Wu, Y., Yu, B., et al. (2021). All-day anti-icing/de-icing coating by solar-thermal and electric-thermal effects. *Adv. Mat. Technol.* 6, 2100371. doi:10.1002/admt.202100371

Lo, T. N. H., Lee, J., Hwang, H. S., and Park, I. (2021). Nanoscale coatings derived from fluoroalkyl and PDMS alkoxysilanes on rough aluminum surfaces for improved durability and anti-icing properties. *ACS Appl. Nano Mat.* 4, 7493–7501. doi:10.1021/acsanm.1c01526

Lv, X., Qin, Y., Liang, H., Zhao, B., He, Y., and Cui, X. (2021). A facile method for constructing a superhydrophobic zinc coating on a steel surface with anti-corrosion and drag-reduction properties. *Appl. Surf. Sci.* 562, 150192. doi:10.1016/j.apsusc.2021.150192

Ma, X., Gao, L., Zhang, J., and Zhang, L.-C. (2017). Fretting wear behaviors of aluminum cable steel reinforced (ACSR) conductors in high-voltage transmission line. *Metals* 7, 373. doi:10.3390/met7090373

Maghsoudi, K., Momen, G., Jafari, R., and Farzaneh, M. (2018). Direct replication of micro-nanostructures in the fabrication of superhydrophobic silicone rubber surfaces by compression molding. *Appl. Surf. Sci.* 458, 619–628. doi:10.1016/j.apsusc.2018.07.099

Maruvada, P. S. (2000). *Corona performance of high-voltage transmission lines*. Baldock, United Kingdom: Research Studies Press.

Megala, V., and Pugazhendhi Sugumaran, C. (2020). Enhancement of corona onset voltage using PI/MWCNT nanocomposite on HV conductor. *IEEE Trans. Plasma Sci. IEEE Nucl. Plasma Sci. Soc.* 48, 1122–1129. doi:10.1109/TPS.2020.2979843

Megala, V., and Sugumaran, C. P. (2019). Application of PI/MWCNT nanocomposite for AC corona discharge reduction. *IEEE Trans. Plasma Sci.* 47, 680–687. doi:10.1109/TPS.2018.2877581

Menati, A., and Xie, L. (2021). "A preliminary study on the role of energy storage and load rationing in mitigating the impact of the 2021 Texas power outage," in 2021 North American Power Symposium (NAPS), College Station, TX, USA, 14-16 November 2021, 1–5. doi:10.1109/NAPS52732.2021.9654452

Meng, X., Mei, H., Zhu, B., Yin, F., and Wang, L. (2022). Influence of pollution on surface streamer discharge. *Electr. Power Syst. Res.* 212, 108638. doi:10.1016/j.epsr.2022.108638

Nasser, E. (1972). Contamination flashover of outdoor insulation. *Electrotekink Autom. (ETZ-A)* 93, 321–325.

Nayak, S. R., Mohana, K. N. S., Hegde, M. B., Rajitha, K., Madhusudhana, A. M., and Naik, S. R. (2021). Functionalized multi-walled carbon nanotube/polyindole incorporated epoxy: An effective anti-corrosion coating material for mild steel. *J. Alloys Compd.* 856, 158057. doi:10.1016/j.jallcom.2020.158057

Nikravesh, B., Ramezanzadeh, B., Sarabi, A. A., and Kasiriha, S. M. (2011). Evaluation of the corrosion resistance of an epoxy-polyamide coating containing different ratios of micaceous iron oxide/Al pigments. *Corros. Sci.* 53, 1592–1603. doi:10.1016/j.corsci.2011.01.045

Olad, A., Maryami, F., Mirmohseni, A., and Shayegani-Akmal, A. A. (2021). Potential of slippery liquid infused porous surface coatings as flashover inhibitors on porcelain insulators in icing, contaminated, and harsh environments. *Prog. Org. Coatings* 151, 106082. doi:10.1016/j.porgcoat.2020.106082

Patil, D., Aravindan, S., Sarathi, R., and Rao, P. V. (2021). Fabrication of self-cleaning superhydrophobic silicone rubber insulator through laser texturing. *Surf. Eng.* 37, 308–317. doi:10.1080/02670844.2020.1780673

Peng, W., Gou, X., Qin, H., Zhao, M., Zhao, X., and Guo, Z. (2018). Creation of a multifunctional superhydrophobic coating for composite insulators. *Chem. Eng. J.* 352, 774–781. doi:10.1016/j.cej.2018.07.095

Peng, W., Gou, X., Qin, H., Zhao, M., Zhao, X., and Guo, Z. (2019). Robust Mg(OH)2/epoxy resin superhydrophobic coating applied to composite insulators. *Appl. Surf. Sci.* 466, 126–132. doi:10.1016/j.apsusc.2018.10.039

Pfeiffer, M., and Franck, C. M. (2015). Impact of conductor surface type and rain intensity on HVDC corona losses. *IEEE Trans. Power Deliv.* 30, 2284–2292. doi:10.1109/TPWRD.2015.2424315

Popoola, A. P. I., Aigbodion, V. S., and Fayomi, O. S. I. (2016). Anti-corrosion coating of mild steel using ternary Zn-ZnO-Y2O3 electro-depositon. *Surf. Coatings Technol.* 306, 448–454. doi:10.1016/j.surfcoat.2016.05.018

Pu, L., Qian, S., Xu, Y., Xie, X., and Cao, X. (2011). "Prevention measures for flashover performance of insulators under icing conditions on 330kV overhead transmission lines," in 2011 Annual Report Conference on Electrical Insulation and Dielectric Phenomena, Cancun, Mexico, 16-19 October 2011, 387–389. doi:10.1109/CEIDP.2011.6232676

Pylarinos, D., Siderakis, K., and Thalassinakis, E. (2015). Comparative investigation of silicone rubber composite and room temperature vulcanized coated glass insulators installed in coastal overhead transmission lines. *IEEE Electr. Insul. Mag.* 31, 23–29. doi:10.1109/MEI.2015.7048134

Qin, Y., Xu, Z., Jia, Z., Guan, Z., Wang, L., and Zhang, R. (2009). "An application of RTV with different conductivities in anti-icing," in 2009 IEEE 9th International Conference on the Properties and Applications of Dielectric Materials, Harbin, China, 19-23 July 2009, 41–44. doi:10.1109/ICPADM.2009.5252512

Shao, Y., Jia, C., Meng, G., Zhang, T., and Wang, F. (2009). The role of a zinc phosphate pigment in the corrosion of scratched epoxy-coated steel. *Corros. Sci.* 51, 371–379. doi:10.1016/j.corsci.2008.11.015

Shreepathi, S., Bajaj, P., and Mallik, B. P. (2010). Electrochemical impedance spectroscopy investigations of epoxy zinc rich coatings: Role of Zn content on corrosion protection mechanism. *Electrochimica Acta* 55, 5129–5134. doi:10.1016/j.electacta.2010.04.018

Sun, J., He, D., Li, Q., Zhang, H., and Liu, H. (2020). Wettability behavior and anti-icing property of superhydrophobic coating on HTV silicone rubber. *AIP Adv.* 10, 125102. doi:10.1063/5.0029398

Swift, D. A., Reynders, J. P., Engelbrecht, C. S., and Fierro-chavez, J. L. (2000). *Polluted insulators : A review of current knowledge*. Paris: Cigré.

Tan, X., Huang, Z., Jiang, L., Xiao, T., Wang, Y., Yang, X., et al. (2021). A simple fabrication of superhydrophobic PVDF/SiO2 coatings and their anti-icing properties. *J. Mater. Res.* 36, 637–645. doi:10.1557/s43578-020-00034-z

Tourkine, P., Le Merrer, M., and Quéré, D. (2009). Delayed freezing on water repellent materials. *Langmuir* 25, 7214–7216. doi:10.1021/la900929u

Ujah, C. O., Popoola, A. P. I., and Popoola, O. M. (2022). Review on materials applied in electric transmission conductors. *J. Mat. Sci.* 57, 1581–1598. doi:10.1007/s10853-021-06681-9

Vazirinasab, E., Jafari, R., and Momen, G. (2019). Evaluation of atmospheric-pressure plasma parameters to achieve superhydrophobic and self-cleaning HTV silicone rubber surfaces via a single-step, eco-friendly approach. *Surf. Coatings Technol.* 375, 100–111. doi:10.1016/j.surfcoat.2019.07.005

Volpe, A., Gaudiuso, C., Di Venere, L., Licciulli, F., Giordano, F., and Ancona, A. (2020). Direct femtosecond laser fabrication of superhydrophobic aluminum alloy surfaces with anti-icing properties. *Coatings* 10, 587. doi:10.3390/coatings10060587

Wang, G., Zhou, W., Zhou, J., Wang, M., Zhang, Y., and Qiang, H. (2021). Superhydrophobic silicone rubber surface prepared by direct replication. *Surf. Eng.* 37, 278–287. doi:10.1080/02670844.2020.1776669

Wang, H., Xu, J., Du, X., Du, Z., Cheng, X., and Wang, H. (2021). A self-healing polyurethane-based composite coating with high strength and anti-corrosion properties for metal protection. *Compos. Part B Eng.* 225, 109273. doi:10.1016/j.compositesb.2021.109273

Wang, L., Liu, L., Fu, X., Mei, H., and Guan, Z. (2016). "Influences of transmission tower anticorrosive coatings on electrical performance of composite insulator," in 2016 IEEE Conference on Electrical Insulation and Dielectric Phenomena (CEIDP), Toronto, ON, Canada, 16-19 October 2016, 834–836. doi:10.1109/CEIDP.2016.7785642

Wang, P., Yao, T., Li, Z., Wei, W., Xie, Q., Duan, W., et al. (2020). A superhydrophobic/electrothermal synergistically anti-icing strategy based on graphene composite. *Compos. Sci. Technol.* 198, 108307. doi:10.1016/j.compscitech.2020.108307

Wei, X., Jia, Z., Sun, Z., Farzaneh, M., and Guan, Z. (2016). Effect of the parameters of the semiconductive coating on the anti-icing performance of the insulators. *IEEE Trans. Power Deliv.* 31, 1413–1421. doi:10.1109/TPWRD.2014.2337012

Wei, X., Jia, Z., Sun, Z., Guan, Z., and Macalpine, M. (2014). Development of anti-icing coatings applied to insulators in China. *IEEE Electr. Insul. Mag.* 30, 42–50. doi:10.1109/MEI.2014.6749572

Wei, X., Jia, Z., Sun, Z., Liao, W., Qin, Y., Guan, Z., et al. (2012). Study of anti-icing performance of insulator strings bottom-coated with semiconductive silicone rubber coating. *IEEE Trans. Dielectr. Electr. Insul.* 19, 2063–2072. doi:10.1109/TDEI.2012.6396966

Xu, L., Liu, F., Liu, M., Wang, Z., Qian, Z., Ke, W., et al. (2019). Fabrication of repairable superhydrophobic surface and improved anticorrosion performance based on zinc-rich coating. *Prog. Org. Coatings* 137, 105335. doi:10.1016/j.porgcoat.2019.105335

Xu, P., Ma, Y., Zhu, J., Zhao, L., Shen, B., and Bian, X. (2022). Effect of TiO 2 coating on the surface condition and corona characteristics of positive DC conductors with particle matters. *High. Volt.* 7, 147–157. doi:10.1049/hve2.12128

Xu, X. (2015). *The development and analysis of shot peening process to improve the aluminum conductor steel reinforced corrosion resistance*. [master's thesis]. Jinan: University of ShanDong.

Xu, Z., and Li, R. (2013). Research on the anti-corona coating of the power transmission line conductor. *Energy Power Eng.* 5, 148–150. doi:10.4236/epe.2013.54B028

Yan, X., Li, J., Li, L., Huang, Z., Hu, J., and Lu, M. (2016). An OH-PDMS-modified nano-silica/carbon hybrid coating for anti-icing of insulators part ii: Anti-icing performance. *IEEE Trans. Dielectr. Electr. Insul.* 23, 2165–2173. doi:10.1109/TDEI.2016.7556491

Yang, C., Wang, F., Li, W., Ou, J., Li, C., and Amirfazli, A. (2015). Anti-icing properties of superhydrophobic ZnO/PDMS composite coating. *Appl. Phys. A* 122, 1. doi:10.1007/s00339-015-9525-1

Yi, Y., Zhang, C., and Wang, L. (2016). Positive dc corona inception on dielectric-coated stranded conductors in air. *IET Sci. Meas. &. Technol.* 10, 557–563. doi:10.1049/iet-smt.2015.0260

Yuan, Y., Xiang, H., Liu, G., and Liao, R. (2021). Fabrication of phase change microcapsules and their applications to anti-icing coating. *Surfaces Interfaces* 27, 101516. doi:10.1016/j.surfin.2021.101516

Yuan, Z., Tu, Y., Li, R., Zhang, F., Gong, B., and Wang, C. (2022). Review on the characteristics, heating sources and evolutionary processes of the operating composite insulators with abnormal temperature rise. *CSEE J. Power Energy Syst.* 8, 910–921. doi:10.17775/CSEEJPES.2019.02790

Zhang, B., Yang, X., Yang, W., Liu, B., Ai, W., and Ma, J. (2016). "The study on the applicability of aluminum conductor carbon core in the high incidence area of galloping for transmission lines," in 2016 IEEE International Conference on High Voltage Engineering and Application (ICHVE), Chengdu, China, 19-22 September 2016, 1–4. doi:10.1109/ICHVE.2016.7800927

Zhang, X., Cotton, I., Li, Q., Rowland, S. M., Emersic, C., Lian, C., et al. (2022). Experimental verification of the potential of superhydrophobic surfaces in reducing audible noise on HVAC overhead line conductors. *High. Volt.* 7, 692–704. doi:10.1049/hve2.12200

Zhang, X., Lian, C., Emersic, C., and Cotton, I. (2019). "Acoustic noise emitted from overhead line conductors with superhydrophobic coating," in 2019 IEEE Electrical Insulation Conference (EIC), Calgary, AB, Canada, 16-19 June 2019, 87–90. doi:10.1109/EIC43217.2019.9046573

Zhang, Z., Jiang, X., Sun, C., Hu, J., Huang, H., and Gao, D. W. (2012). Influence of insulator string positioning on AC icing flashover performance. *IEEE Trans. Dielectr. Electr. Insul.* 19, 1335–1343. doi:10.1109/TDEI.2012.6260009

Zhao, Q., Liu, Z., Yu, P., Chen, L., and Guan, F. (2022). "Review of transmission line icing and anti-icing technologies," in *The proceedings of the 16th annual conference of China electrotechnical society lecture notes in electrical engineering*. Editors X. Liang, Y. Li, J. He, and Q. Yang (Singapore: Springer Nature), 1224–1232. doi:10.1007/978-981-19-1870-4_129

Zhu, L., Xue, J., Wang, Y., Chen, Q., Ding, J., and Wang, Q. (2013). Ice-phobic coatings based on silicon-oil-infused polydimethylsiloxane. *ACS Appl. Mat. Interfaces* 5, 4053–4062. doi:10.1021/am400704z

Zhu, M.-X., Song, H.-G., Li, J.-C., Xue, J.-Y., Yu, Q.-C., Chen, J.-M., et al. (2021). Superhydrophobic and high-flashover-strength coating for HVDC insulating system. *Chem. Eng. J.* 404, 126476. doi:10.1016/j.cej.2020.126476

Zhuang, J., Liu, P., Dai, W., Fu, X., Lin, H., Zeng, W., et al. (2010). A novel application of nano anticontamination technology for outdoor high-voltage ceramic insulators. *Int. J. Appl. Ceram. Technol.* 7, E46–E53. doi:10.1111/j.1744-7402.2009.02395.x

Zhuang, J. (2010). *Structure modification of TiO2 film and its novel application for promoting the anti-contamination performance of high voltage outdoor insulators*. [master's thesis]. Fuzhou: University of Fuzhou.

Zuo, Z., Liao, R., Guo, C., and Zhao, X. (2015). "Fabrication and anti-icing property of superhydrophobic coatings on insulator," in 2015 IEEE Conference on Electrical Insulation and Dielectric Phenomena (CEIDP), Ann Arbor, MI, USA, 18-21 October 2015, 161–164. doi:10.1109/CEIDP.2015.7352052

Zuo, Z., Song, X., Liao, R., Zhao, X., and Yuan, Y. (2019). Understanding the anti-icing property of nanostructured superhydrophobic aluminum surface during glaze ice accretion. *Int. J. Heat Mass Transf.* 133, 119–128. doi:10.1016/j.ijheatmasstransfer.2018.12.092